ANALYSIS OF N- AND O-LINKED GLYCOPEPTIDES

by

LILY BIRX

(Under the Direction of Ron Orlando)

ABSTRACT

A glycoprotein is a glycoconjugate in which a protein has one or more glycans covalently attached to a polypeptide backbone, usually via N- or O- linkages. This modification can affect the structure, function, interaction, and folding of proteins. Glycosylation is crucial for physiological and pathological cellular functions.[1] Specific N- and O-linked glycoprotein changes are associated with disease progression and the identification of these glycoproteins has potential for use in disease diagnostics, prognosis, and treatment.[2,3] For example, Immunoglobulin G (IgG), the most common serum antibody, is N-glycosylated and studies have established IgG glycosylation as a key regulator of humoral immune activity.[4,5,6,7]

The biological significance of IgG and other glycoproteins makes the development of accurate methods to analyze them vital. Structural analysis of glycoproteins is generally performed with or without release of the glycan modification. A proteolytic digestion can be performed on a glycoprotein to produce glycopeptides. In addition, N-glycans can be released by Peptide-N4-(N-acetyl-beta-glucosaminyl)asparagine amidase (PNGase F).

Liquid chromatography paired with mass spectrometry (LC-MS) is commonly used for the analysis of proteins, glycoproteins, and glycans. The emergence of Tandem MS (MS/MS) and hydrophilic interaction liquid chromatography (HILIC) methodologies have assisted in the

identification and characterization of glycoproteins. The current work presented here utilizes HILIC-LC-MS methods to address various gaps in the field by increasing the depth of information obtained from experiments, including investigating retention behavior, reducing the identification of false positives, and determining kinetics of PNGase F deglycosylation for complete glycan release. The purpose of the work presented here is multifaceted: first, to use HILIC to analyze the separation of O-mannose glycosylated peptides and investigate their retention behavior to facilitate faster, and more confident identification and characterization of unknowns. Second, a novel HILIC-LC-MS method, n-Asp and i-Asp to reduce false positives (NIFP), was proposed to reduce interferences in glycosylation site mapping.[8] Third, the kinetics of PNGase F deglycosylation reactions performed on intact and trypsin digested IgGs were investigated for the development of efficient methods for accurate quantitation. The effect of different PNGase F enzyme preparations on the kinetics of deglycosylating Human Serum IgGs was also investigated.

INDEX WORDS: Liquid Chromatography, Mass Spectrometry, Glycoprotein Characterization, Glycosylation, Glycosylation Site Mapping, Post-Translational Modifications, N-Glycosylation, O-Glycosylation, Retention Time Prediction, Deamidation, Hydrophilic Interaction Liquid Chromatography

ANALYSIS OF N- AND O-LINKED GLYCOPEPTIDES

by

LILY BIRX

BS, University of Alabama at Birmingham, 2018

A Dissertation Submitted to the Graduate Faculty of The University of Georgia in Partial Fulfillment of the Requirements for the Degree

DOCTOR OF PHILOSOPHY

ATHENS, GEORGIA

2022

ANALYSIS OF N- AND O-LINKED GLYCOPEPTIDES

by

LILY BIRX

Major Professor:	Ron Orlando
Committee:	Jon Amster
	Lance Wells

Electronic Version Approved:

Ron Walcott
Vice Provost for Graduate Education and Dean of the Graduate School
The University of Georgia
August 2022

DEDICATION

To my dad, Dan Birx.

ACKNOWLEDGEMENTS

To Ron, you always mention how you believe the most important responsibility of your role is mentoring and developing future scientists. As someone on the receiving end of that mentorship, I appreciate you taking on that role and truly making sure that everyone leaves your lab a better scientist than they enter. Thank you for helping me reach my goals.
I could not have done this, learned all that I have, or become the scientist I am without your support and advice. You taught me to think deeply, question everything, and be the harshest critic of my own data. You allowed me to become an independent researcher who can approach and solve problems myself, but also were always there to answer questions and talk through problems. I'll look back fondly at graduate school, and I have you to thank for that.

To Lance Wells and Jon Amster, I really appreciate both of you being on my committee. The classes you both taught provided me with the fundamental knowledge that I applied to my research, and provided a scope of the field at-large, which I learned to see myself in. Thank you both for your help over the years and for providing unique perspectives and ideas for me to apply in my research.

To Barry Boyes, thank you for sharing your vast knowledge of chromatography with me, and for always being willing to jump on a zoom call to answer questions or listen to my chromatography woes.

To Tyler Fletcher, thank you, I truly lucked out by having you as the 'older, more experienced' graduate student in the lab, and you taught me so much. You showed me how to use a wrench to fix LCs and to see every challenge as an opportunity. Like Ron, you gave me the

opportunity to work independently, solve my problems, and take charge of my research, while also being there to provide guidance. I'm grateful our times at UGA overlapped because I would not have become the researcher I am today without you.

To Star Scott, of UGA Green Labs, thank you for all your help in making my research sustainable, something I used to think was impossible. I appreciate you sharing your vast knowledge of sustainability with me, mentorship, and for cheering me on to become the best version of myself (while also advocating for self-care and balance).

To Avery Smith and Zach McQueen, thank you for your friendship over these years, without it, graduate school would not have been possible.

To Lauren Pepi, thank you for always being a listening ear, and for all your help navigating graduate school.

To the Complex Carbohydrate Research Center for providing me with the resources necessary for me to obtain this degree in an unbelievable facility. To Carl Bergman, thank you for your help, guidance, and wisdom over the years.

To Amy Davis and Monica Bledsoe, friends like you two are hard to come by, I'm so grateful that our paths crossed. Our friendships are the best thing that ever came from me hosting CGSO tailgates.

Sugar free Red Bull, I also could not have done this without you. #givesyouwiiings

TABLE OF CONTENTS

Page

LIST OF TABLES

Page

LIST OF FIGURES

Page

CHAPTER 1

INTRODUCTION

Glycoproteins are proteins that have oligosaccharide chains (glycans) covalently attached to polypeptide amino acid side chains, usually via N- and O-linkages, and play vital roles in a wide range of biological processes, as well as in disease genesis and progression.[1] Changes in specific N- and O-linked glycoprotein are associated with disease progression and the identification of these glycoproteins has potential for use in disease diagnostics, prognosis, and treatment.[2,3] For example, Immunoglobulin G (IgG), the most common serum antibody, is N-glycosylated and studies have established IgG glycosylation as a key regulator of humoral immune activity.[4,5,6,7]

Structural analysis of glycoproteins is generally performed with or without release of the glycan modification. A proteolytic digestion can be performed on a glycoprotein to produce glycopeptides. In addition, N-glycans can be released by Peptide-N4-(N-acetyl-beta-glucosaminyl)asparagine amidase (PNGase F). PNGase F, which cleaves the linkage between the asparagine residue and the innermost N-acetylglucosamine (GlcNAc) of all N-glycans except those containing a 3-linked fucose attached to the core GlcNAc. The analysis of glycopeptides is beneficial as the glycan is still attached, providing site information that can be used to determine the glycan's function.

Due to their great biological importance, the development of fast and accurate methods to analyze glycoproteins is of the upmost importance. Liquid chromatography paired with mass spectrometry (LC-MS) is a powerful tool for the analysis of glycoproteins, proteins, and glycans.

Hydrophilic Interaction Liquid Chromatography (HILIC) is the preferred separation method of glycopeptides and has also been shown to chromatographically separate different glycoforms which is key in characterizing the glycans that occupy a specific site.

The current work presented here utilizes HILIC-LC-MS methods to address various gaps in the field by increasing the depth of information obtained from experiments, including investigating retention behavior, reducing the identification of false positives, and determining kinetics of PNGase F deglycosylation for complete glycan release.

Chapter 3 details the investigation of the HILIC retention behavior of O-mannose glycopeptides. The separation of six O-mannose glycopeptides was observed and the glycopeptides were able to be resolved from each other, and from the native, unmodified peptide. Retention coefficients for O-mannose and extended structures were calculated. The separation of GlcNAc linkage isomers in O-mannose glycopeptides was also observed, and the HILIC retention contribution for both was determined. Retention behavior prediction improves data analysis methods as it allows for quicker data analysis and facilitates the identification of unknowns. The calculation of O-mannose glycan coefficients allows for the prediction of retention time for any O-mannose glycopeptide consisting of the investigated sugars on any peptide sequence, when combined with previous HILIC peptide retention model.[9]

Chapter 4 proposes an alternative to the current methodology used to locate sites of N-linked glycosylation on a protein. Researchers commonly identify sites of N-linked glycosylation on a protein through the identification of deamidated sites after releasing the N-glycans with peptide-N-glycosidase F (PNGase F). A current method to locate sites of N-linked glycosylation on a protein involves the identification of deamidated sites after releasing the glycans with PNGase F. This protocol involves a proteolytic digest and then PNGase F deglycosylation, both

performed in buffer conditions with a pH of 7.8, an optimum range for both enzymes. However, a potential interference to this method of N-glycosylation site mapping is the chemical deamidation of Asn residues, which occurs spontaneously, has been observed to occur in conditions of proteolytic digestion and pH deglycosylation, and can result in false positives. To overcome these interferences, a novel HILIC-LC-MS method, n-Asp and i-Asp to reduce false positives (NIFP), was proposed.[8]

Chapter 5 highlights the investigation into solving an age-old question, on whether researchers need to perform a trypsin digest before performing a PNGase F deglycosylation on IgGs. Currently, researchers either perform PNGase F deglycosylation on intact or trypsin digested IgGs. Those who perform PNGase F deglycosylation on trypsin digested IgGs argue that proteolysis is needed to reduce steric hindrance while the other states that this step is not needed. There is minimal experimental evidence supporting either assumption. Thus, the kinetics of a PNGase F deglycosylation reaction for intact IgGs and IgG glycopeptides was investigated, and statistically significant differences between the rates were determined.

Chapter 6 expands on previous research and investigates the kinetics of PNGase F deglycosylation reaction for multiple preps, where three PNGase F enzyme preparations were compared (one amidase and two recombinant versions). The importance of obtaining complete glycan release for accurate quantitation led us to determine if there was a difference in the rate of deglycosylation between the three PNGase F preps. Statistically significant differences in the rate of deglycosylation performed using three different PNGase F enzyme preps on trypsin digested IgGs was determined.

CHAPTER 2

LITERATURE REVIEW

Liquid Chromatography

Liquid chromatography (LC) is a technique used to separate a sample into its individual parts, based on the chemical or physical interactions of the sample with the mobile phase and stationary phases. Initially, discovered as means to separate colored compounds, LC has modernized over the years. Modern high-performance liquid chromatography (HPLC) encompasses the same principles as early LC techniques but provides greater separation efficiency, versatility, and speed to keep up with contemporary demand and is used for the analysis of pharmaceuticals, metabolites, and biological samples.[10,11,12] In HPLC, the sample is first placed on a tray for automatic injection into the column. Solvent is continually pumped through the column, and the separated compounds are continuously monitored by a detector as they leave the column. The resulting detector signal plotted against time is referred to as a chromatogram. Nowadays, a computer automates the processes and HPLC is characterized by the use of high-pressure pumps for faster separations, re-usable and effective columns for enhanced separations, for an enhanced separation and more precise process.

General Description

The interactions utilized in a separation can be chemical, with an analyte adsorbing to an adsorbent surface, or physical, where a small analyte easily penetrates a porous particle. In LC, components within a mixture are separated in a column based on each component's affinity for the mobile phase.[13] Most mobile phases are made up of acetonitrile, methanol, and/or water. Ion

pairing reagents can be added to the mobile phase to improve the selectivity of the separation. Ammonium formate and formic acid are common mobile-phase modifiers in LC-MS based proteomic workflows.[14] In the infancy of LC analysis, the mobile phase composition remained constant, or isocratic, throughout a separation but as researchers began to analyze more complicated samples, they needed to vary mobile phase composition throughout a separation in the form of gradients.[15,16]

In LC, the stationary phase directly interacts with the sample through various modes of interaction based on affinity, size, and electrostatic interactions. Stationary phases are typically made of porous, microscopic particles that are packed into a column, one of the most popular particles used are core-shell particles, also referred to as superficially porous particles (SPPs). SPPs have a solid, impermeable inner core of silica covered by a thin, porous shell also made out of silica, they provide highly efficient and fast separations with low back-pressure.[17,18,] The type of adsorbent material making up the particles of the stationary phase is crucial for efficient separation of compounds in a mixture. [19,20] Today, inorganic materials including silica, graphite, and metal oxides are widely used in research applications. Silica has become one of the most widely used HPLC packing materials due to its good mechanical strength, high chemical and thermal stability, controllable pore structure and surface area, and surface rich in silanol groups.[19,21,22] The physical characteristics of the particles must also be considered. The particle size, mean diameter of the particle used to pack a column, affects the distance and time necessary for a molecule to partition between the mobile and stationary phases. While the pore size influences whether a molecule can diffuse into and out of particles. The utilization of a small particle size provides better efficiencies as there is less peak dispersion across a wide range of flow rates. While the pore size must be large enough to allow interactions between the molecule

and the stationary phase. Smaller pore sizes (80 - 120Å) are best for molecules with a molecular weight up to 2000 Da.[23]

After the appropriate stationary phase and mobile phase is chosen for the separation. There are two main factors that contribute to how well compounds are separated by chromatography: efficiency, and resolution. A column's efficiency is referred to in terms of band broadening, which describes how a group of the same type of analyte moves apart as it moves through a column. The efficiency of a column is commonly defined by the number of plates (N) a column has. Thus, the more plates a column has, the more efficient the column is, and the separation between the two solutes is greater. The plate count of a column is related to the mobile phase used and nature of the solute. The theoretical plate height (H) can be calculated using N and column length (L) to measure column efficiency (Equation 1). Column length is fixed so many plates result in a small value of theoretical plate height, resulting in a more efficient column.

$$H = \frac{L}{N} \quad \text{(Eq. 1)}$$

In 1956, Van Deemter defined the relationship between column efficiency and theoretical plate height to measure the equilibration of a sample between stationary and mobile phases (Equation 2).

$$H = A + \frac{B}{u} + Cu \quad \text{(Eq. 2)}$$

In this equation, there are three terms that influence the height of a plate: Eddy diffusion (A), Longitudinal diffusion (B), resistance to mass transfer (C), and average mobile phase velocity (u).[24] In order to have a high efficiency separation, the plate height needs to be low, requiring the factors that influence band broadening to be minimized. Eddy diffusion is a constant, that is independent of flow rate and accounts for the effects of multi-path flows in a

column, including the effects of injection and detection. In packed columns, multiple distinct routes (channels) exist through the column packing, resulting in band spreading. Longitudinal diffusion accounts for the effect of a solute undergoing diffusional broadening within the mobile phase.[25] The final term, resistance to mass transfer represents the movement of an analyte between the stationary and mobile phases, or a transfer of masses between the phases. Some analytes will move from phase to phase while others will predominately be in the mobile phase. This increases the band broadening, but can be reduced through the use of lower flow rates, smaller particles, or increasing temperature.[26,27,28] The mobile phase velocity (flow rate) used in a separation is important as it affects band broadening through its impact on longitudinal diffusion and resistance to mass transfer. The flow rate can vary from in the range milliliters to nanoliters, with sensitivity of detection increasing at lower flow rates. However, too low of flow rate, increases the longitudinal diffusion factor, as the analyte spends more time on the column, which increases plate height. While a flow rate that is too high, results in adsorption of the analyte to the stationary phase, leaving some of the sample behind. Thus, the flow rate must be optimized to improve column efficiency, while maintaining a reasonable separation time.[10]

Column efficiency is necessary in determining the degree of separation within a column but being able to separate two adjacent peaks is equally as important. The extent of this separation is referred to as resolution, which is defined as the difference in retention times between two peaks, divided by the combined widths of the elution peaks (Equation 3).

$$R_s = \frac{2[(t_R)_B - (t_R)_A]}{W_B + W_A} \text{ (Eq. 3)}$$

Where B is the species with the longer retention time, A is the species with the shorter retention time, and t_r and W are the retention time and elution peak width, respectively. A resolution greater than one indicates that the peaks can be differentiated successfully. However, a resolution value of 2 to 3 is desired.[29,16]

Types of Liquid Chromatography

From the development of chromatography in the 1900s and until the introduction of reverse phase (RP) chromatography in the 1970s, Normal phase (NP) chromatography was the method of choice. NP-LC utilizes a polar, inorganic stationary phase and a less-polar, water-free mobile phase. In NP-LC, the stationary phase is more polar than the mobile phase, allowing more-polar solutes to be preferentially retained. After the development of RP-LC, NP-LC is less common but is still useful for analytical separations by thin-layer chromatography (TLC), purification of crude samples, and for the separation of very polar samples that are poorly retained and separated by RP-LC.[16]

Nowadays, RP-LC is the most common HPLC separation technique and is the first choice for the separation of both neutral and ionic samples. RP-LC utilizes a non-polar, hydrophobic stationary phase such as C8 or C18, and a polar mobile phase, typically a mixture of water and either acetonitrile or methanol. It is commonly used in the field due to its convenience, robustness, and versatility. Over the course of gradient elution, very polar molecules interact more strongly with the polar mobile phase, thus these compounds are less retained and leave the column first. Whereas less polar compounds prefer the nonpolar stationary phase and are retained longer and elute when the mobile phase becomes more organic. RP-LC is ideal for the separation of hydrophobic compounds, including peptides. While, very hydrophilic glycans

interact minimally with the non-polar stationary phase in RP-LC, resulting in in-adequate resolution of isobaric glycoforms of glycopeptides.[16,30]

In contrast to RP-LC, hydrophilic interaction liquid chromatography (HILIC) is an alternative HPLC mode for separating polar compounds. HILIC, coined by Alpert in 1990, is historically referenced as a variant of NP-LC, but the separation mechanism utilized in HILIC is more complicated than in NP-LC.[31] There are many advantages to HILIC chromatography; (1) it allows for the retention of compounds in complex systems that elute near the void in RP-LC, (2) polar samples have good solubility in the aqueous mobile phase used in HILIC, (3) costly ion-pair reagents are not required, and it can be coupled to mass spectrometry.[32] In HILIC, a non-polar mobile phase and a polar, hydrophilic stationary phase are used. Gradient elution in HILIC begins with a low-polarity organic solvent and elutes polar analytes by increasing the polar aqueous content. HILIC works by retaining polar compounds into a water-rich layer that is formed at the surface of the silica particle because of a polar stationary phase. HILIC is the separation mode of choice for highly hydrophilic and amphiphilic compounds that are too polar to be well retained in RP-LC but have insufficient charge to allow effective electrostatic retention in ion-exchange chromatography.[33,34,35]

Detectors in Liquid Chromatography

The chromatographic detector is a transducer that converts a chemical or physical property of an eluted analyte into an electrical signal that can be related to analyte concentration. There are two types of detectors used in liquid chromatography: destructive and non-destructive. Destructive detectors perform continuous transformation of the column effluent, with a destructive process (burning, evaporating, or mixing with reagents), with a subsequent measurement of a physical property of the resulting material. When a destructive detector is

used, the original sample cannot be recovered after analysis, the sample is destroyed during analysis. A mass spectrometry detector is an example of a destructive detector. Non-destructive detectors directly measure a property of the column eluent and provide greater analyte recovery. Thus, the sample is not destroyed when analyzed by a non-destructive detector. Ultraviolet (UV), fluorescence, and refractive index (RI) detectors are examples of non-destructive detectors.[36,37,38] Mass spectrometry and UV detectors are the most commonly used LC detectors for the analysis of glycopeptides. The UV detector measures a sample's absorption of light at different wavelengths and provides a continuous signal that is used to quantify the amount of chromophoric compounds in the sample.

Retention Time Modeling

Retention modeling is done in proteomic analysis where the individual contributions of amino acids to the retention of a peptide are analyzed to accurately predict when peptides elute. Such models have been made for both RP and HILIC chromatography, in which each amino acid has a coefficient that describes the extent of its hydrophilicity/hydrophobicity.[9,39,40] These coefficients are them summed for a particular peptide and can be used to calculate the retention time for any peptide sequence. Models have also been derived to predict the retention coefficients of post-translational modifications including glycosylation, oxidation of methionine, and deamidation.[41,42] The implementation of predicted retention times in peptide and glycopeptide analysis adds an additional selection, ultimately aiding in their characterization and identification, while reducing false discovery rates.[43]

Mass Spectrometry

Mass Spectrometry (MS) measures the mass-to-charge (m/z) ratio of ions, which can be used to calculate the exact molecular weight and determine the structure of a molecule. Mass

Spectrometers consist of an ion source that converts analyte molecules into gas-phase ions, a mass analyzer under an ultra-high vacuum that separates ionized analytes based on their m/z, and a detector. The detector electronically produces a signal representative of the separated ions and records the number of ions at each m/z value.[44] The results are viewed as a mass spectrum, a plot of intensity as a function of m/z ratio. Low operating pressures (high vacuum) is utilized in mass spectrometry to reduce the chance of ions colliding with other molecules in the mass analyzer, as these collisions can interfere with the mass spectrum.

Ionization Techniques

The development of electrospray ionization (ESI) and matrix-assisted laser desorption/ionization (MALDI) revolutionized protein analysis using MS. ESI and MALDI are referred to as "soft ionization techniques" as ion formation does not lead to a significant loss of sample integrity, making them applicable to protein and glycoprotein analysis. In both ESI and MALDI, peptides are converted into ions by either addition or loss of one or more than one proton.

ESI produces ions using an electrospray in which a high voltage is applied to a liquid to create an aerosol. Ionic species in solution can be analyzed by ESI-MS with increased sensitivity and neutral species can be converted to ionic form in solution or gaseous phase by protonation or cationization. There are three main steps to utilized in ESI: (1) dispersal of a fine spray of charged droplets followed by (2) solvent evaporation, and (3) ion ejection from the highly charged droplets. In ESI, a nebulizing gas, typically nitrogen, is used to shear around the eluted sample solution, and enhances a higher sample flow rate. The nebulizing gradient is also typically heated as well as the ESI source. The charged droplets generated at the end of the electrospray tip, pass down a pressure gradient and potential gradient towards the analyzer

reason of the mass spectrometer.[45] The formation of ions requires ample desolvation, requiring organic solvents to be mixed with water. There are two main theories to explain ion formation in ESI: the charge residue model (CRM) and the ion evaporation model (IEM). IEM proposes that as the droplet reaches a certain radius the field strength at the surface of the droplet becomes large enough to assist in the field desorption of solvated ions. While CRM suggests that electrospray droplets undergo evaporation and fission cycles, eventually producing progeny drops that contain one analyte ion or less. The gaseous ions form after the remaining solvent molecules evaporates, leaving the analyte with the charges that the droplet carried. The efficiency of generating the gaseous ions in ESI varies depending on the compound structure, the solvent used, and instrumental parameters.[46,47,46]

MALDI is another soft ionization technique used to study biological samples. In MALDI, the sample is mixed with an energy absorbent matrix, that crystallizes and entraps the sample upon drying. The sample-matrix is ionized by a laser beam, and desorption and ionization with the laser beam generates singly charged protonated ions from analytes in the sample.[48]] The matrix used in MALDI is vital for the successful generation of ions. 2,5-dihydroxybenzoic acid (DHB) and α-cyano-4-hydroxycinnamic acid (CHCA) are two commonly used matrices in proteomics analysis.[49] The charged analytes resulting from ESI and MALDI are then detected and measured using different types of mass analyzers.

Mass Analyzers

There are many configurations of mass analyzers, including quadrupole, ion trap, and time-of-flight (TOF). In the 1950s, Wolfgang Paul and his student Helmut Steinwedel first conceived the quadrupole mass filter (QMF), which consists of four cylindrical rods, set parallel to each other. Opposite rods are electronically connected with direct current (DC) and radio

frequency (RF) voltages. If the RF voltage is the only one applied, a wide range of m/z ions will traverse through the quadrupole. When a DC voltage is superimposed onto the RF voltage, ions of a specific m/z can be tuned to traverse the quadrupole, while ions of higher or lower m/z values will be lost by collisions with the quadrupoles through unstable trajectories. The mass range can be scanned to transmit ions of increasing m/z to acquire a mass spectrum, this is done by increasing the DC and Rf voltages while keeping their ratio constant. QMF's allow one mass channel at a time to reach the detector as the mass range is scanned, leading them to be described as scanning instruments.[50,51,52]

Quadrupole ion-trap (QIT) mass analyzers are similar to QMF but differ as the ions are trapped in stable orbits and are then sequentially ejected. There are two types of QIT, three-dimensional (3D) and linear. The 3D-QIT consists of three hyperbolic electrodes: a donut-shaped ring electrode, an entrance endcap electrode, and the exit endcap electrode. Ions enter and are trapped in the space between the electrodes by DC and RF potentials, the RF potential is then altered to produce instabilities in the ion trajectories to axially eject the ions into the detector in increasing m/z value. LIT differs from QMF as two electrodes are placed at the ends of the quadrupole to trap ions, as ions enter the trap, the front plate potential is ramped up to "trap", then the rear plate potential is reduced to attract ions to exit for further analysis.[53,54,55,56] In both designs, an inert buffer gas, typically helium, is added into the trap to dampen the energy of the ions, to reduce unwanted collisions. LIT's are noted to have higher ion storage volumes and enhanced sensitivity for externally ejected ions than QIT. Overall ion traps are advantageous due to their high ion storage capability, high scan rate, and simplicity.

A linear time-of-flight (TOF) mass analyzer separates ions based on their velocity as they travel through a flight region, called the flight tube. An ion's trajectory depends on its

momentum and kinetic energy imparted by an applied pulse acceleration voltage (pusher) and its m/z ratio. Ions with a lower m/z value will travel the fastest, arriving at the detector first, while ions with larger m/z will travel slower and arrive at the detector last. Linear TOF mass analyzers experience poor mass resolution caused by differences in start times and locations of ions being accelerated as well as different kinetic energies and initial ion orientation. However modern instrumental design has been optimized to overcome these disadvantages, mainly in the development of reflectron time-of-flight mass spectrometers (RTOF-MS). Reflectrons utilize a retarding electrostatic field, where pulsed ions penetrate until they lose their kinetic energy and travel in the opposite direction to reach a detector. The reflectron corrects for the distribution of kinetic energies of analyzed ions.[57] Newer instruments include double reflectrons, where ions are pushed, reflected by the first reflectron opposite the pusher, and then by a second reflectron, then by the first reflectron again before arriving at the detector. To correct for differing initial position and velocity of ions, a delayed extraction technique can be implemented where ions generated from the ion source are delayed momentarily before they are accelerated through the flight tube.[58] A buffer gas is also utilized to reduce the kinetic energy of ions entering into the flight tube.[59] TOF mass analyzers, with a reflectron, are advantageous due to their high sensitivity and ion transmission, fast scan speed, and excellent mass range, and tend to have a higher resolution than quadrupole or ion-trap mass analyzers.

Tandem Mass Spectrometry

Tandem mass spectrometry (MS/MS, MS^2) is a two-step technique to break down selected ions (precursor ions) into fragments (product ions). First, m/z are isolated then fragmented by a chemical reaction (dissociation), the fragment ions are then used to characterize and identify the precursor ion. Collision-induced dissociation (CID) is a common dissociation

method used in MS/MS, where gas-phase peptide/protein cations are internally heated by multiple collisions with rare gas atoms (helium, argon, or nitrogen). During this collision process, a fraction of the ion's kinetic energy is transferred into internal energy, determining its dissociation into various fragment ions; the extent of fragmentation depends on the total internal energy of the excited ion. CID results in peptide backbone fragmentation of the carbon-nitrogen bond and the formation of a series of b- and y-fragment ions.[60] Multiple dissociation processes exist and produce varying fragmentation patterns, such as electron-transfer dissociation (ETD).[61] MS/MS can be conceived in two ways: tandem-in-space and tandem-in-time. Tandem-in-space instruments utilize two mass analyzers in series; thus, the different stages of the process occur sequentially in separate physical regions. Whereas, in Tandem-in-time instruments the different MS/MS stages are carried out successively inside the same physical space but separately in time.[62,63]

A triple quadrupole (QQQ) mass analyzer is a popular tandem-in-space instrument, consisting of two quadrupoles (Q1 and Q3) in series with a non-mass-resolving RF only quadrupole between them, acting as a cell for collision-induced dissociation. The first quadrupole (Q1) operates to select a precursor ion m/z, the second quadrupole operates with an RF potential to allow ion transmission while at a higher pressure for fragmentation, and the third quadrupole operates to select fragment m/z. [64,65] Triple quadrupole instruments have four MS/MS scan modes: precursor ion scan, fragment ion scan, neutral ion scan, and selected reaction monitoring (SRM). In each MS/MS scan modes, the collision cell is used for fragmentation. Precursor scans are set up to utilize Q1 as a mass analyzer to scan for precursor ions while Q3 acts as a filter, only allowing a specific m/z through. Thus, allowing for identification of precursor ions that produce a particular fragment. Fragment ion scans, also

known as product ion scans, occur when Q1 is set to only allow the transmission of one m/z, and Q3 scans for the fragment ions. In a neutral ion scan, Q1 and Q3 are scanned simultaneously at the same rate but with differing DC/RF ratios, the difference in m/z filtered between each is equal to a neutral loss of interest. Selected reaction monitoring (SRM), also referred to as multiple reaction monitoring (MRM) operates Q1 to isolate a precursor ion and Q3 to isolate a fragment ion, allowing for a targeted approach to specifically look for peptides of interest and their corresponding fragments, providing increased specificity and sensitivity for quantitation. Overall, QQQ instruments provide high duty cycle; the proportion of time that ions are accepted from a continuous ion source, correlating to high sensitivity as few ions are wasted, and are preferentially used for quantitation analysis.

Quadrupole time-of-flight (QTOF) instruments are another popular tandem-in-space instrument. This configuration is similar to a QQQ but differ in that the third quadrupole is replaced can by a TOF mass analyzer. This setup provides many benefits to sensitivity, mass resolution, and mass accuracy in both precursor (MS1) and product ion (MS/MS) modes, and is ideal in the analysis of unknowns.[66]

Ion Detection

A key component in MS systems is the detector used to convert a current of mass separated ions into measurable signal. Electron multipliers are one of the most common detectors due to their high gain and low noise. Electron multipliers consist of a vacuum-tube structure that multiplies incident charges, in which a single electron is bombarded on a secondary-emissive material, causing the ejecting of secondary electrons. These electrons are accelerated through an applied electric field to the next metal plate and induce secondary emission of more electrons.

This process is repeated multiple times, resulting in many electrons being collected by a metal anode. There are three geometries: discrete dynode, continuous dynode, and microchannel plates.

In a discrete dynode electron multiplier, the electrons are sequentially attracted to individual charged plates called dynodes. The electrons cascade down the plates which are inside a glass or ceramic tube that has a resistive coating, and as one hits a plate it emits additional electrons.[67] A continuous dynode system utilizes a horn-shaped funnel of glass coated with a thin film of semiconducting materials.[68] The multiplication principle is similar to the discrete dynode but electrons are emitted from the continuous inner surface of the horn instead of plates. A microchannel plate is an 2-dimensional parallel array consisting of very small continuous-dynode electron multipliers.[69,70]

Glycoproteins

Liquid chromatography paired with mass spectrometry (LC-MS) methods are utilized in the analysis and characterization of proteins and their modifications. Post-translational modifications (PTMs) are amino acid modifications in some proteins after their biosynthesis and include phosphorylation, glycosylation, acetylation, methylation, and ubiquitination. PTMs are highly dynamic and have been known to regulate many cellular and biological processes.[71] Glycosylation is one of the most common PTMs in proteins. At least 50% of human proteins are glycosylated, with some estimating that it is closer to 70%.[72,73] Glycosylation is an important and highly regulated mechanism of secondary protein processing within cells, playing a vital role in determining protein structure, function, and stability.[74] A glycoprotein is a glycoconjugate in which a protein has one or more glycans covalently attached to a polypeptide backbone, usually via N- or O- linkages. Specific N- and O-linked glycoprotein changes are associated with disease

progression and the identification of these glycoproteins has potential for use in disease diagnostics, prognosis, and treatment.[2,1,3]

N- and O-linked Glycoproteins

N-linked linked glycoproteins consist of a glycan covalently attached to an Asparagine (Asn) residue by a N-glycosidic bond. The minimal amino acid sequence to receive an N-glycan is Asn-X-Ser/Thr in which "X" is any amino acid, except Proline (Pro). However, not all Asn residues in this sequon are N-glycosylated. All N-glycans contain a core structure consisting of two N-Acetyl Glucosamines (GlcNAc) and three Mannoses (Man), and all Eukaryotic N-glycans begin with a GlcNAc β1-linked to the Asn residue.[75] There are three types of N-glycans: (1) Oligomannose, in which only Man residues extend the core; (2) Complex, in which "antennae" initiated by GlcNAc extend the core; and (3) Hybrid, where Man extends the Manα1-6 arm of the core and one or two GlcNAcs extend the Manα1-3 arm. The GlcNAc branches of complex and hybrid N-glycans can be modified by Galactose (Gal), then N-Acetylneuraminic acid (Neu5Ac) or N-Glycolylneuraminic acid (Neu5Gc).[75]

A glycan covalently attached to a Serine (Ser), or Threonine (Thr) is referred to as an O-glycoprotein. There is no consensus sequence or single common core structure in O-glycosylation. O-linked glycosylation is commonly found in the serine- and threonine-rich regions of mucin and mucin-like proteins.[76] There are also several types of non-mucin glycosylation including O-GlcNAcylation[77], O-mannosylation[78], and O-fucosyslation[79].

Immunoglobulins

Immunoglobulins (Igs) are soluble serum glycoproteins utilized in the adaptive immune system to identify and neutralize pathogens. Immunoglobulin G (IgG) is the most abundant antibody in the human body, composed of four subunits, made up of two heavy chains and two

light chains.[80] IgGs are involved in multiple humoral immune processes including antigen neutralization, complement activation and complement dependent cytotoxicity (CDC), and antibody-dependent cell-mediated cytotoxicity (ADCC).[81] There are four subclasses of IgGs (IgG1, IgG2, IgG3, and IgG4), that differ in their constant regions, particularly in their hinges and upper CH2 domains.[4] All IgGs are N-glycosylated at aspargine-297 (Asn-297) in the CH_2 domain of the crystallizable fragment (Fc) part of the heavy chains. In human IgG, most of the Fc glycans are complex biantennary structures with a high degree of heterogeneity, due to the presence or absence of different terminal sugars. Previous studies have shown that IgG glycosylation modulates IgG effector functions and is involved in disease development and progression.[82]

Biotherapeutics

IgGs are able to be recombinantly produced and used as biotherapeutics. Some of the most common and popular drugs on the market, are biotherapeutics, including Humira, Avastin, Epogen, and Rituxan. Glycosylation is a key factor determining the pharmacological properties of biotherapeutics, including their stability, solubility, bioavailability, pharmacokinetics, and immunogenicity. Hence, an increased attention is directed at optimizing the glycosylation properties of biotherapeutics.[83]

Biotherapeutic drugs are synthesized through recombinant protein expression in a host cell, typically produced in non-human mammalian cells. Chinese Hamster Ovary (CHO) cells are the most commonly used cells to produce biologics.[84] Many mammalian cell expression systems used can produce biotherapeutic glycoproteins that are mostly decorated with human-like glycans, but in some cases non-human glycans can be presented. There are two common examples of non-human glycan structures being presented at the terminal, most exposed position.

First, human N-glycans lack the terminal Gal 1-3Gal (α-Gal) modification; and second, they do not contain the non-sialic acid N-glycolylneuraminic acid (Neu5Gc). Instead of containing Neu5Gc, humans have an increased abundance of its precursor N-acetylneuraminic acid (Neu5Ac). Most humans have circulating antibodies specifically targeting Neu5Gc and α-Gal, risking immunogenicity of biotherapeutics carrying such non-human glycan epitopes.[85,86,87] An example of this α-Gal immunogenicity/contamination was first seen in the biotherapeutic drug Cetuximab, a chimeric mouse-human IgG1 monoclonal antibody directed against the epidermal growth factor receptor, for the treatment of colorectal and squamous-cell cancer, approved by the US Food and Drug Administration (FDA) in 2003. Once on the market, a high rate of hypersensitivity reactions occurred upon the first application of cetuximab in the southeastern US federal states. The immunogenicity caused by the presence of non-human glycans on biotherapeutic drugs highlights the great need to analyze the glycosylation present.[88,89,90]

Glycoprotein Characterization using LC-MS

The biological significance of these glycans and glycoproteins makes the development of accurate methods to analyze them vital. LC-MS is commonly used for the analysis of glycoproteins. Glycoprotein and protein identification in MS can be carried out in the form of whole-protein analysis ("top-down" proteomics) or analysis of enzymatically or chemically induced peptides ("bottom-up" proteomics).[91] In glycoproteomic analysis, a bottom-up approach is preferred due to the greater separation efficiency, simpler spectral interpretation, among other benefits.[92] A benefit of the bottom-up approach is the ability to "shotgun" analyze complex protein mixtures, where a proteolytic digest is performed on a protein altogether and the contents are investigated. This bottom-up approach has successfully identified proteins in complexes,

organelles, whole cells, and tissues. This approach also provides information about modification sites.[53]

In a bottom-up approach, prior to proteolytic digestion, the protein must be denatured to allow the protease to work efficiently. This can be done through the addition of denaturing agents such as surfactants, sodium dodecyl sulfate (SDS), urea, and guanidine hydrochloride (GHCl), to the initial buffer solution.[93] However, these surfactants are not ideal for MS systems. Denaturation can also be achieved by breaking the disulfide bridges in the protein through reduction with dithiothreitol (DTT) and then alkylation with iodoacetamide (IDA) to prevent reformation of the disulfide bonds.[92,94] Next, the proteolytic digestion is typically performed in-solution with a protease enzyme, that cleaves the glycoprotein into glycopeptides. There are many proteases available, including Trypsin, Chymotrypsin, Pepsin, and Proteinase K, differing by their cleavage selectivity and specificity.[95] Trypsin is the most commonly used, due to its known specificity, as it cleaves at the C-terminal side of Arginine (Arg) and Lysine (Lys) residues.[96]

Structural analysis of glycoproteins is generally performed with or without release of the glycan modification, the former approach is referred to as “glycomics” and the latter is referred to as “glycoproteomics”. The glycomics approach allows for the released glycans to be direct injected into a MS, derivatized, among other analytical methods for in-depth characterization. A majority of N-linked glycans can be released from glycoproteins/glycopeptides with Peptide-N4-(N-acetyl-beta-glucosaminyl)asparagine amidase (PNGase F), which cleaves the bond between the first GlcNAc residue of the glycan and the glycosylated asparagine. PNGase F is not able to cleave N-linked glycans from glycoproteins when the innermost GlcNAc residue is linked to an α1-3 Fucose residue. However, a downside of the glycomics approach is that site-specific

information is lost as the glycan is released from the protein. Whereas, in the glycoproteomics approach, the glycan is not released, and the glycosidic bond is kept intact throughout analysis to obtain information about glycosylation sites and site occupancies.[92] Glycosylation site mapping can be performed on glycopeptides, and aids in the identification of a glycosylation site, which can provide an indication of the function of the glycan.

Glycopeptides and released glycans can be analyzed by LC-MS methodologies to obtain information on the structure of the peptide, composition of the glycan, and site information. However, glycopeptide analysis can be complicated due to microheterogeneity, which is a diversity of glycans occupying a protein's glycosylation sites, as well as the presence of structural and linkage isomers, all contributing complexity.[93] The introduction of tandem mass spectrometry (MS/MS) has shown to be a vital tool for glycoproteomic analysis as it is able to provide structural information to aid in identification. When glycopeptides are subjected to CID, fragment ions are formed, corresponding to low molecular weight oxonium ions such as 163 m/z (Hex^+), 204 m/z ($HexNAc^+$), 366 m/z ($Hex\text{-}HexNAc^+$), and 292 m/z ($Neu5Ac^+$). In addition, glycopeptides fragment to produce glycosidic cleavage ions of the Y- and B-ion type, resulting in consecutive losses of 162 Da (Hex), 203 Da (HexNAc), and 291 Da (Neu5Ac) that are observable in the CID spectra. Together, observation of these oxonium and glycosidic cleavage ions aid in the identification and verification of a glycopeptide.[97,98,99,100] Separation by Liquid chromatography is implemented before MS aids in isomeric identification.[101] Hydrophilic Interaction Liquid Chromatography (HILIC) is the preferred separation method of glycopeptides and has also been shown to chromatographically separate different glycoforms which is key in characterizing the glycans that occupy a specific site.

CHAPTER 3

INVESTIGATING THE RETENTION BEHAVIOR OF O-MANNOSE GLYCOPEPTIDES

Birx, L., Praissman, J., Live, D., Orlando, R., Wells, L. To be submitted to *Journal of Biomolecular Techniques*

Abstract

O-mannose glycosylation is a common post-translational modification (PTM) and can alter the overall structure, polarity, and function of proteins. In Hydrophilic interaction liquid chromatography (HILIC), the polar glycan interacts with the polar stationary phase, offering the ability to separate a glycosylated peptide from its native form. Thus, changes made to either moiety will alter the chromatographic behavior of the glycopeptide. HILIC has also been shown to separated glycopeptide isomers. Glycopeptide isomers are often differentially associated with various biological processes. In this paper, the retention behavior of previously uninvestigated O-mannose glycopeptides was investigated. Retention coefficients for O-mannose and extended structures are calculated. The separation of β-1,2-linked GlcNAc and β-1,4-linked GlcNAc on POMGNT1 and POMGNT2 O-mannose glycopeptides was demonstrated. Retention behavior prediction improves data analysis methods as it allows for quicker data analysis and facilitates the identification of unknowns.

Introduction

Glycosylation of extracellular and membrane proteins is an important post-translational modification (PTM) involved in protein stability, quality control, cell-surface retention, and ligand interactions.[74] The post-translational glycosylation of select proteins by O-mannose is a conserved modification from yeast to humans and has been shown to be necessary for proper development and growth.[102] O-Linked mannose (O-mannose) glycans are initiated by covalent linkage of mannose to the hydroxyl oxygen of a serine or threonine amino acid residue by protein O-mannosyltransferases (PMTs) using dolichol-phosphate-B-D-mannose as a donor.[103,104] A variety of glycan structures can be formed through the extension of O-mannose by

the addition of other monosaccharides, including hexoses and N-acetylglucosamines (HexNAcs), and functional groups.

There are four major classifications of O-mannose-initiated glycans (Fig 1), the last three have been reviewed in-depth by Praissman and Wells.[105] The retention behavior of six O-mannose glycopeptides was investigated. There structures are shown as Fig 2. In this paper, POMG1/POMG2 is referred to as 1-Man.

The ability to resolve glycosylated peptides from their native forms greatly facilitates analysis as it enables glycan characterization while connected to a peptide tag that provides the glycan's location. The hydrophilic nature of glycans results in their inability to be separated in Reversed Phase-Liquid Chromatography (RP-LC), where hydrophobic interaction drives the retention. In contrast, glycans interact strongly with the stationary phases used in HILIC, allowing for the separation of peptide/glycopeptide pairs. In general, the retention of glycans and glycopeptides on HILIC is determined by the hydrophilicity of the analyte, which is influenced by structural features such as size, charge, composition, linkage, and oligosaccharide branching.[106] HILIC has also been shown to separate glycopeptide isomers, including determining α2-3/2-6 sialic acid (SA) linkage isomers of N-glycans.[107]

Here, the retention behavior of previously uninvestigated O-mannose glycopeptides is observed. The separation of β-1,2-linked GlcNAc and β-1,4-linked GlcNAc on POMGNT1 and POMGNT2 O-mannose glycopeptides was also investigated. This work expands upon previous studies that calculated the retention coefficients that represent the hydrophilicity of O-linked N-acetylgalactosamine (O-GalNAc), O-linked N-acetylglucosamine (O-GlcNAc), and O-fucose.[108] Wherein, Dextran is utilized as a retention calibrant, allowing for peptide and glycopeptide

retention to be expressed in glucose units (GUs) facilitating comparison of retention across different LC-mass spectrometry (MS) systems.

Materials and Methods

Glycopeptides

Synthetic peptide-glycopeptide pairs were obtained from the Wells lab at the Complex Carbohydrate Research Center (Athens, GA, USA). The peptide sequence is PKRVRRQIHAT*PTPVTAIGPP, where the * indicates the O-man residue. In addition, the peptide's N-term is acetylated and C-term is a carboxamide, the synthesis of the O-man peptide and subsequent work with it is described in the following paper.[109]

Protein Digestion

Synthetic peptide and glycopeptides were reduced using 200 mM dithiothreitol (DTT) and alkylated using 1M iodoacetamide (IDA), both purchased from Sigma Aldrich (St. Louis, MO, USA) to a final concentration of 5 mM DTT and 8 mM IDA. Sequencing grade trypsin purchased from Promega (San Luis Obispo, CA, USA) was added at 20:1 (w/w, protein/trypsin) for incubation overnight at 37°C.

LC-MS/MS settings and instrumentation

Data were acquired using a Synapt G2 (Waters Corporation, Milford, MA, USA) in series with a 1100 Series LC System (HP, Santa Clara, CA, USA). Samples were suspended in 80% acetonitrile and 20% H_2O and separated using a HALO Penta-HILIC column packed with 2.7 um-diameter superficially porous particles (Advanced Materials Technology, Wilmington, DE, USA) at 60°C. The gradient elution conditions used a linear increase in aqueous solvent from 20% to 50% over 30 minutes at 0.200 mL/min flow rate. The mobile phases contained 0.1% formic acid (Sigma-Aldrich) in acetonitrile, and the aqueous solvent contained 50 mM

ammonium formate (Sigma-Aldrich) and 0.1% formic acid in deionized water. The settings for the mass spectrometer included the use of an inclusion list of the glycopeptide masses to preferentially select these ions for fragmentation using collision-induced dissociation, and the resulting MS/MS spectra was recorded.

Selection of peptides for prediction model and post-run data analysis

Retention times were determined manually from RAW files using the apex of peaks displayed in MassLynx software (Waters Corporation) and resulting MS/MS data were visually inspected for fragmentation that was consistent with peptide assignments. Skyline software was utilized to analyze data.[110]

Results and Discussion

The Separation of Glycopeptides from their Native Forms

The ability to resolve the six O-mannose modified glycopeptides from the native species is shown by the HILIC chromatogram of the peptide QIHAT*PTPVTAIGPP, where the * indicates the glycosylated site (Fig. 3). All peaks are baseline resolved, highlighting the ability of the HILIC column to separate the species with the hydrophilic O-mannose modifications. Retention times in minutes were converted to GUs from procainamide-labeled Dextran samples ran immediately before and after the peptide/glycopeptide samples. The GU value is calculated by fitting a fifth order polynomial distribution curve to the dextran ladder, then using this curve to allocate GU values from retention times.[111] This approach allows the model to be universal and used regardless of LC-MS system used, as long as dextran is ran before/after the samples.

The retention time of the unmodified form of the peptide was determined experimentally and also predicted from a previously made model (Table 1). This peptide model is based on amino acid composition and is able to sum amino acid coefficients related to their

hydrophilicities with an intercept to predict retention.[9] A deviation of 1.67 GU was observed between the experimental retention time of the unmodified peptide and the predicted value. The experimental retention time in GU was used for all calculations.

All six O-mannose modified glycopeptides not only are resolved from their native, unmodified form, but also are resolved from each other. Table 2 shows the retention times in GU, structures, and elution order of the O-mannose glycopeptides and native/unmodified version of the peptide. For the 1-Man glycopeptide, the addition of 1 mannose sugar residue drives the interaction with the water-rich layer of the stationary phase, resulting in a later elution time compared to the native/unglycosylated peptide. In POMGNT1, the addition of the second moiety continues to increase the overall hydrophilicity of the peptide more than the addition of one mannose in the 1-Man structure, shown by its later elution time. TMEM5 is the latest eluting O-mannose glycopeptide, as it contains the most monosaccharides as well as 2 phosphates. As more monosaccharides are added, the glycopeptide retains longer on the HILIC column due to the increased hydrophilicity from the additional polar groups. In HILIC, the separation of glycopeptide species is strongly dictated by the number of polar groups, which leads to rather predictable and intuitively interpretable elution patterns.[106]

There are two species containing 1 mannose and 1 GlcNAc residue differing only by linkages, POMGNT1 has a β-1,2 linked GlcNAc while POMGNT2 has a β-1,4 linked GlcNAc. The ability to resolve the POMGNT1 species with the β-1,2 linkage from the POMGNT2 species with the β-1,4 linkage is shown by the HILIC chromatogram (Fig. 4). The difference between POMGNT1 (RT – 13.64 min and POMGNT2 (RT – 14.14 min) is 0.50 min, 0.42 GU. The isomeric glycans are being resolved based on a ratio of β-1,2 to β-1,4 linkages present in the glycoforms, with the β-1,2-linked isomers eluting before the β-1,4 glycoforms. This suggests that

the linkage of the GlcNAc residue affects the number of exposed -OH groups to the water-rich layer of the stationary phase. The increase in the number of exposed -OH increases the overall hydrophilicity of the residue. The POMGNT2 with β-1,4 linkage elutes later due to the increased hydrophilicity compared to POMGNT1 (β-1,2 linkage). The separation of branch position of sialic acid of glycopeptides using HILIC separation has been extensively reported previously.[112,107] To our knowledge this is the first description of HILIC separation of β-1,2-linked GlcNAc and β-1,4-linked GlcNAc O-mannose glycopeptides.

Coefficients of O-mannose Glycans

The prediction of retention for peptides with O-mannose modifications can further the identification process and aid in the identification of unknowns. In total, the retention behavior of three peptides containing each modification were investigated. The three species include the native peptide, the native peptide with pyroglutamylation at the N-terminus, and the native peptide with one missed cleavage. The retention times in GU for the glycopeptides is shown in Table 3.

Coefficients were calculated to determine how the modifications influence the overall hydrophilicity of the peptides, analysis of retentions times with and without modifications were used to derive coefficients (Table 4). The coefficients represent the hydrophilicity of the modification and are expressed in GU, and their high coefficient values were expected because of the size and polar characteristics of the sugar additions.

Though the retention behavior of mannose was investigated, a coefficient was calculated for hexoses (mannose, glucose, galactose, etc.), as they only differ by the position of some of its hydroxyl groups. Thus the isomeric glycans should have similar coefficients, consistent with experimental observations.[108] However, the separation of β-1,2- and β-1,4-GlcNAc linkage

isomers, as shown previously, highlighted that linkage isomers do not have the same retention behavior. Thus, a coefficient for each HexNAc linkage isomer was calculated.

The strong hydrophilic phosphate group is the main contributor in the average coefficient of a β-1,3-HexNAc plus phosphate sugar. As expected, phosphorylated peptides and glycopeptides retain strongly under typical HILIC conditions. The negative charge of the phosphate group increases the hydrophilicity of the glycan, thus resulting in a later retention time and higher coefficient than HexNAc alone.

Ribitol has the largest coefficient for monosaccharide additions studied here, suggesting that the contribution of ribitol adds hydrophilicity to the glycopeptide. Ribitol is pentose sugar alcohol formed by the reduction of ribose.[113] Ribitol has a linear structure compared to the pyranose ring-shape of hexoses, allowing the -OH groups of ribitol to be more solvent accessible than those of hexoses, increasing the interaction with the HILIC stationary phase, resulting in a longer retention time and retention coefficient.

The calculation of retention coefficients for these O-mannose glycans allows for future retention predictions to be made. The ability to predict the retention of O-mannose glycans provides important benefits to analysis methods. The combination of O-mannose glycan coefficients and previous HILIC peptide retention model[114], allows for the prediction of retention time for any O-mannose glycopeptide consisting of the investigated sugars on any peptide sequence. It allows for retention information to be obtained for glycans that have not been analyzed previously, eliminating the need for prior experimental data. This is particularly useful for the analysis of O-mannose glycans as standards are difficult to synthesize and are not readily available. In addition, once retention information is obtained, the identification of glycans can be made with greater confidence. Retention prediction provides quicker data analysis as peptides

can be identified from their m/z ratio as well as their retention time, altogether eliminating the need for database searching. Software database searches typically produce several possible identities with erroneous or incomplete assignments occurring with regularity, and the ability to predict the retention behavior can assist by confirming the appropriate identity. O-mannose glycans are also typically not included in software database searches. Overall, retention prediction of O-mannose glycopeptides allows for quicker and more confident data analysis.

Conclusion

The attachment of O-mannose glycans to a peptide increased the overall hydrophilicity and causes the glycosylated species to be more retained on a HILIC column. The six O-mannose glycopeptide species were able to be resolved from each other, from the unglycosylated peptide, and from baseline. In addition, the novel HILIC separation of β-1,2-linked GlcNAc and β-1,4-linked GlcNAc O-mannose glycopeptides was observed. The implementation of a previously derived HILIC peptide retention model to provide the retention contribution of a peptide sequence allows for the HILIC retention behavior of any O-mannose glycopeptide to be determined if the glycan structure matches one studied. This work shows the ability of the HILIC column to separate these six O-mannose glycopeptides and unmodified species in a predictable manner, which allows for easier identification, characterization, and quantification.

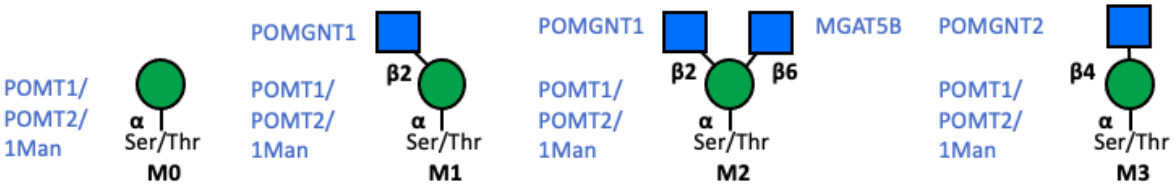

Figure 1. Four classifications of core O-mannose structures.

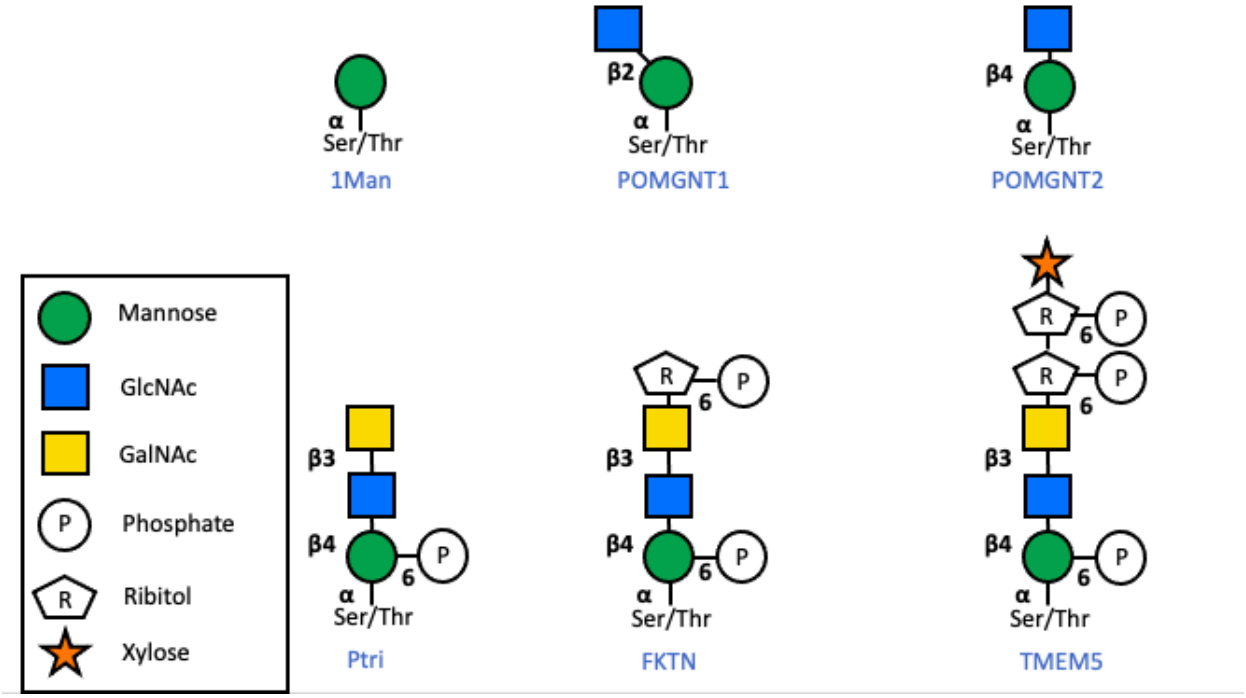

Figure 2. The structures of the six O-mannose glycopeptides whose retention behavior was investigated is presented here.

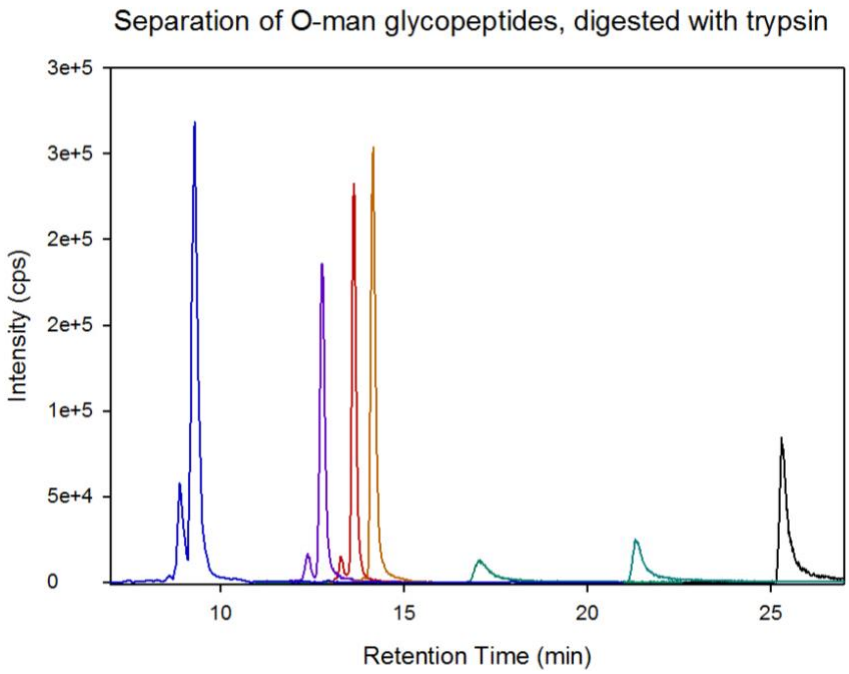

Figure 3. Separation of six O-mannose glycopeptides and native/unmodified version of the peptide QIHAT*PTPVTAIGPP, where the * indicates the glycosylated site. Extracted ion chromatograms of each o-mannose species (No mannose/unglycosylated (blue)– $[749.9]^{++}$, 1-Man (purple) $[830.93]^{++}$, POMGNT1 (red)/POMGNT2 (orange) - $[932.47]^{++}$, Ptri (green) – $[1073.99]^{++}$, FKTN (teal)– $[1181.01]^{++}$, TMEM5 (black) – $[903.03]^{+++}$).

Table 1. Experimental Retention Times of Unmodified, Synthetic Peptide Compared with Predicted Retention Values.						
Source	Sequence	Monoisotopic Mass (Da)	Average Exp RT, min	Average Exp RT, GU	Predicted RT, GU	Deviation, GU
Synthetic peptide from Well's lab	QIHATPTPVTAIGPP	1498.81	9.98	2.71	4.38	1.67

Table 2. Retention Behavior and Elution Order of O-mannose Modified Peptide QIHAT*PTPVTAIGPP (* indicates the glycosylated site).			
Sugar	Structure	Retention Time (GU)	Retention Time difference from preceding glycopeptide (GU)
Unmodified/no sugar	-	2.71	-
1man	1 mannose	3.66	0.95
pomgnt1 (β2)	1 mannose, 1 β-1,2-linked GlcNAc	3.78	0.12
pomgnt2 (β4)	1 mannose, 1 β-1,4-linked GlcNAc	4.20	0.42
Ptri	1 mannose, 1 β-1,4-linked GlcNAc, 1 β-1,3-linked GalNAc, and 1 1-6 linked phosphate attached	6.46	2.26
FKTN	1 mannose, 1 β-1,2-linked GlcNAc, 1 β-1,3-linked GalNAc, 1 phosphate, and 1 ribitol	9.13	2.67
TMEM5	1 mannose, 1 β-1,2-linked GlcNAc, 1 β-1,3-linked GalNAc, 2 phosphates, 2 ribitols, and 1 xylose	17.51	8.21

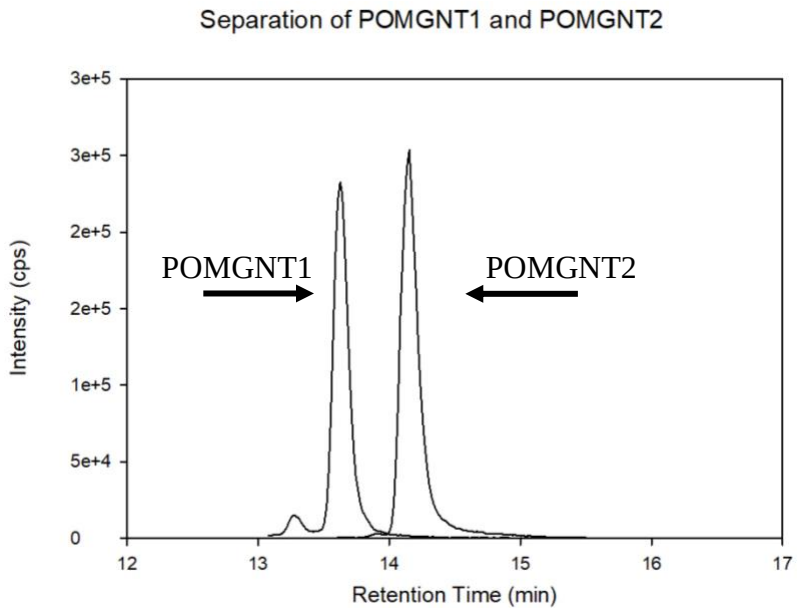

Figure 4. Separation of POMGNT1 (β-1,2 linkage, retention time: 13.64 min) and POMGNT2 (β-1,4 linkage, retention time: 14.14 min) of the tryptic peptide QIHAT*PTPVTAIGPP, where the * indicates the glycosylated site. Figure shows extracted ion chromatograms of POMGNT1/2 ($[932.47]^{++}$) species.

Table 3. Retention Times of Unmodified and O-mannose Modified Glycosylated Peptides.			
Peptide	QIHATPTPVTAIGPP	**Q**IHATPTPVTAIGPP	RQIHATPTPVTAIGPP
Sugar	Average RT in GU		
none	2.71	1.37	4.34
1man	3.66	2.23	5.24
pomgnt1 (β2)	3.78	2.73	-
pomgnt2 (β4)	4.20	2.85	5.73
Ptri	6.46	5.13	8.34
FKTN	9.13	7.70	11.06
TMEM5	17.51	16.39	-

Table 4. Retention Coefficients of O-mannose Glycans.				
	QIHATPTPVTAIGPP	**Q**IHATPTPVTAIGPP	RQIHATPTPVTAIGPP	
	Average Coefficient in GU			Avg
Hexose	0.950	0.856	0.892	0.90
HexNAc (β2)	0.423	0.499	0.374	0.43
HexNAc (β4)	0.536	0.625	0.494	0.56
HexNAc (β3) + Phosphorylation	2.261	2.278	2.637	2.40
Ribitol	2.675	2.572	2.692	2.65

CHAPTER 4

REDUCING INTERFERENCES IN GLYCOSYLATION SITE MAPPING

Birx, L., Harvey, A., Popov, M., Orlando, R. Reducing Interferences in Glycosylation Site Mapping. *Journal of Biomolecular Technique*. 2022. Reprinted here with permission of publisher.

Abstract

A current method to locate sites of N-linked glycosylation on a protein involves the identification of deamidated sites after releasing the glycans with peptide-N-glycosidase F (PNGase F). PNGase F deglycosylation converts glycosylated asparagine (Asn) residues into aspartic acids (Asp). The 1 Dalton mass tag created by this process is observable by liquid chromatography/tandem mass spectrometry (LC/MS/MS) analysis. A potential interference to this method of N-glycosylation site mapping is the chemical deamidation of Asn residues, which occurs spontaneously and can result in false positives. Deamidation is a pH dependent process that results in the formation of iso-Aspartic Acid (i-Asp) and native Aspartic Acid (n-Asp) by a succinimide intermediate. Whereas PNGase F deglycosylation results in the conversion of the glycosylation Asn residue into n-Asp. N-linked glycosylation sites can thus be identified by the presence of a single chromatographic peak corresponding to an n-Asp residue within the consensus sequence Asn-X-Ser/Thr, while sites of deamidation lead to two chromatographic peaks resulting from the presence of n-Asp and i-Asp. The intent of this study is to alert investigators in the field to the potential and unexpected errors resulting from this phenomenon and to suggest a strategy to overcome this pitfall and limit the number of false positive identifications.

Introduction

Glycosylation is an important and highly regulated mechanism of secondary protein processing within cells, playing a vital role in determining protein structure, function, and stability. N-linked glycosylation of proteins occurs on Asn residues by an N-glycosidic bond. In eukaryotic cells, N-linked glycosylation occurs in a consensus sequence Asn-X-Ser/Thr, where X can be any amino acid except proline.[75] Changes in N-linked glycosylation have been

associated with different diseases including rheumatoid arthritis, type 1 diabetes, Crohn's disease, and cancers, [115,116,117,118,119] indicating the importance for the accurate analytical characterization of this post-translational modification.

Chemical deamidation of Asn residues is a well-known and studied post-translational modification (PTM) in proteins.[120,121] It occurs spontaneously on proteins and peptides and influences several biological processes. Deamidation has been reported to be related to Alzheimer's disease and cataracts[122,123,124] and it has also been thought to function as a "molecular clock" in aging.[125,126] Nonenzymatic deamidation of Asn results in the formation of native Aspartic Acid (n-Asp). Under mildly alkaline conditions, Asn deamidation happens mainly through the formation of a succinimide ring intermediate that is quickly hydrolyzed to n-Asp and iso-Aspartic Acid (i-Asp), with i-Asp predominating in a 1:3 ratio.[121,127,128] This reaction is reversible and occurs at pH > 5 via a base-catalyzed pathway. The deamidation rate can be influenced by several factors related to the protein sequence and environmental changes, such as a temperature, ionic strength, and pH.[129] It has been shown that deamidation of Asn followed by glycine (Gly) or serine (Ser) is predominant due to the small and hydrophilic side chains of these amino acids.[130,131,132] The deamidation rate of peptides increases significantly under conditions typical of tryptic digestion, i.e. incubation in digestion buffers at pH 8 for 8–16 h at 37 °C.[133] Consequently, the conditions used for sample preparation can induce peptide deamidation that is not present in the initial sample.

Identification of deamidated sites by liquid chromatography-tandem MS (LC-MS/MS) is a step in the assignment of N- glycosylation sites after PNGase F deglycosylation. Release of N-linked glycans is commonly done using a glycosidase such as PNGase F.[134]

Peptide-N-glycosidase convert glycosylated Asn residues into Asp, resulting in a mass shift of 1 Da at the site of modification. This leads researchers to assign potential sites of N-linked glycosylation based on the identification of Asp within the consensus sequence Asn-X-Ser/Thr. Mechanistically the enzymatic deglycosylation will only lead to n-Asp, not the mixture of n-Asp/i-Asp produced by chemical deamidation. However, this is not conclusive for assigning potential sites of N-linked glycosylation, as both naturally occurring and experimentally induced deamidation of Asn may convert Asn into n-Asp, resulting in the same 1 Da mass shift.[135]

Attempts in our laboratory to map sites of N-linked glycosylation on HER2 employing PNGase F deglycosylation followed by LC/MS/MS produced puzzling results. Specifically, multiple sites of Asn deamidation were identified but none of these were in the Asn-X-Ser/Thr consensus sequence. Both naturally occurring and experimentally induced deamidation of Asn into n-Asp, results in a 1 Da mass shift, allowing for possible interferences resulting in false positives. This prompted us to investigate the possibility of deamidated peptides being misidentified as sites of N-linked glycosylation during PNGase F deglycosylation and develop a useful approach to differentiate between chemical and enzymatic deamidation.

Materials and Methods

Peptide Digestion

Adalimumab and a glycoprotein consisting of the extra cellular domain of human epidermal growth factor receptor 2 fused with the Fc domain of human IgG1 (HER2-FC) from GlycoScientific (Athens, GA, USA) were first buffer exchanged with 50 mM ammonium bicarbonate (pH 7.8) or 50 mM ammonium acetate (pH 6.8). Then reduced using 200 mM dithiothreitol (DTT) and alkylated using 1M iodoacetamide (IDA), both purchased from Sigma Aldrich (St. Louis, MO, USA), to a final concentration of 5 mM DTT and 8 mM IDA.

Sequencing grade trypsin purchased from Promega (San Luis Obispo, CA, USA) was added at 20:1 (w/w, protein/trypsin) for incubation at 37 °C. After 48 hours passed, the samples were removed and divided in half. One half of the sample was dried down and resuspended in 80% ACN and 20% H_2O. 500 units of PNGase F was used to deglycosylate the other half of the sample and incubated for an additional 48 hours at 37 °C. After a total of 96 hours passed, the sample was removed from the incubator and set on a 100 °C heat block for 5 min to inactivate the PNGase F. The sample was then dried down and resuspended in 80% ACN and 20% H_2O.

LC-MS/MS Settings and Instrumentation

Data were acquired using a 4000 Q Trap (AB Science, Chatham, NJ, USA) with a Nexera UFLC (Shimadzu, Columbia, MD, USA). Peptides were separated using a column 2.1 mm x 150- mm HALO ® Penta-HILIC column packed with 2.7 um diameter superficially porous particles that have a 90 Å pore diameter (Advanced Materials Technology, Wilmington, DE, USA) at 60°C. The mobile phases used in the separation were 0.1% formic acid, 50 mM ammonium formate in water (A) and 0.1% formic acid in acetonitrile (B). The peptides were bound to the column in 82% B and a linear gradient to 54% B over 30 minutes was initiated to elute the peptides. Skyline was used to make a transition list.[110]

Results and Discussion

Recent attempts in our laboratory to map sites of N-linked glycosylation on HER2 protein in breast cancer employing PNGase F deglycosylation followed by LC/MS/MS produced puzzling and ambiguous results. In particular, multiple sites of deamidation, i.e., sites of N-glycosylation, were identified but not found within the Asn-X-Ser/Thr consensus sequence required for N-linked glycosylation.[75] Our interest was in determining whether the analytical approach was defining accurate sites of modification. It was hypothesized that chemical

deamidation could explain the deamidation observed, since deamidation is known to occur at pH 7.8, a common pH for digestion with trypsin and PNGase F. Ambiguities led us to examine the HER2 data in greater detail. The potential for chemical deamidation occurring during deglycosylation was investigated using HILIC-MS to analyze trypsin/PNGase F digested adalimumab.

Deamidation of Asn increases the hydrophilicity of the altered residue, and HILIC polar stationary phases have the potential to separate these changes in hydrophilicity while allowing for quantitation of unmodified species and their modified counterparts.[42] Chromatographic analysis was thus applied to resolving enzymatic and chemical deamidation, as only the later mechanism should result in a mixture of aspartyl isomers with the succinimidyl intermediate, with no such mixture resulting from an enzymatic process. While chemical deamidation is expected to produce a mixture of i-Asp and n-Asp products due to the succinimide intermediate. The mechanism for chemical and enzymatic deamidation through PNGase F deglycosylation is shown in Figure 1. Experiments were performed in both high (pH 7.8) and low (pH 6.8) pH conditions as previous studies have shown that the deamidation rate of peptides increases significantly under conditions typical of tryptic digestion and PNGase F deglycosylation, i.e. incubation in digestion buffers at pH 8 for 8–16 h at 37 °C.[133]

The peptide EEQYNSTYR contains the one site of N-linked glycosylation in Human IgG1, commonly occupied with the A2G0F glycan structure.[136] After 48 hours, the Asn version is only species present at both high and low pH conditions (Fig 2A & 2B) as the presence of the glycan does not allow for deamidation to occur. PNGase was then added to remove the glycan and convert the glycosylated Asn residue into Asp, resulting in a plus one Dalton shift in the peptide's molecular weight. After the addition of PNGase F and a total incubation period of 96

hours, the representative peptide in both the high and low pH conditions, continued to only show one peak (Fig 3A & 3B) corresponding to the n-Asp containing species.

The data demonstrates that PNGase F deglycosylation converts the Asn exclusively to an n-Asp as it does not go through a succinimide intermediate thus leading to only one product. The PNGase F deglycosylation does result in an addition of one Dalton of mass to the peptide's molecular weight but previous data shown highlights that PNGase F deglycosylation is not the only manner leading to Asn deamidation in a sample. Deamidation is a pH dependent process that results in the formation of two peaks, one for the n-Asp and i-Asp versions. Whereas PNGase F deglycosylation results in a one peak from the conversion of the glycosylation Asn residue into n-Asp.

This is highlighted again in the chromatogram of the representative glycopeptide (GHCWGPGPTQCVNCSQFLR) from HER2 (Fig. 4). After 48 hours, PNGase F was added, and the sample was incubated at 37°C for an additional 48 hours. After the addition of PNGase F, removing the glycan attached and converting the Asn to n-Asp, only one peak is observed at 18.9 minutes corresponding to the n-Asp version (Fig 4). The identity of the peptide was also confirmed orthogonally using a HILIC Retention prediction model.[9] The data demonstrates that PNGase F deglycosylation converts the Asn to an n-Asp and thus the i-Asp version is not observed. The single peak corresponding to n-Asp species after PNGase F treatment demonstrates that this position in HER2 is indeed glycosylated.

Analysis of the de-glycosylated peptides led us to investigate sites of deamidation to devise a strategy to differentiate between these two deamidation mechanisms. The VVSVLTVLHQDWLNGK peptide from IgG1 contains an unglycosylated n-Asn in an 'Asn-Gly' site, which are known to be highly susceptible to chemical deamidation. After 48 hours in

pH 7.8 conditions, the formation of n-Asp and i-Asp is observed in this peptide as shown in Figure 5. As determined in a previous study, n-Asp and i-Asp can be chromatographically separate through HILIC[42], as illustrated in Figure 5. The first peak at 11.4 minutes corresponds to amidated Asn. The peak at 12.9 minutes corresponds to n-Asp and the peak at 13.4 minutes corresponds to i-Asp. Previous studies on chemical deamidation have shown that i-Asp is three times more abundant than n-Asp. The ratio of peak abundances of n-Asp and i-Asp in Figure 5 is analogous to this statement.[127,128] The least retained peak is the unmodified form of the peptide, while the peak in the middle is the aspartyl version, and the peak most retained is the isoaspartyl version. The i-Asp version elutes later than the native form due to the hydrophilicity of the modification.[42]

After 48 and 96 hours in pH conditions that mimicked trypsin/PNGase F digestion, the deamidated version of this peptide eluted in two peaks, corresponding to the peptide containing an n-Asp or an i-Asp. These results are consistent with chemical deamidation and demonstrate the chemical deamidation occurs to a significant extent under typical enzymatic deglycosylation conditions. The data demonstrates that deamidation is a pH dependent process and that PNGase F deglycosylation is not the main contributing factor to the deamidation for this peptide which indicates that the peptide is not glycosylated. The assumption that all sites of Asn deamidation resulting from enzymatic digestion/deglycosylation marks an N-linked glycosylation site is not consistent with the results of this experiment.

The current method of identifying N-linked glycosylation sites based on the presence of Asp within the consensus sequence Asn-X-Ser/Thr, requires further identification of aspartyl or isoaspartyl mixtures to differentiate between chemical and enzymatic deamidation. A new method of N-linked glycosylation site identification through Asn deamidation is proposed that

considers both chemical and enzymatic deamidation, n-Asp and i-Asp to reduce false positives (NIFP).

By this proposed NIFP method, N-linked glycosylation sites can be identified by the presence of an n-Asp residue within the consensus sequence Asn-X-Ser/Thr that also chromatographically shows the presence of one peak, corresponding to Asp. The site is considered to be chemically deamidated if the chromatogram shows the presence of two peaks corresponding to the n-Asp and i-Asp.

Conclusion

Naturally occurring and experimentally induced deamidation of Asn can interfere with the identification of N-linked sites of glycosylation. Identification of n-Asp within the consensus sequence Asn-X-Ser/Thr after deglycosylation with PNGase F is not conclusive for assigning potential sites of N-linked glycosylation, as both chemical and enzymatic deamidation of Asn can convert Asn into n-Asp, resulting in the same 1 Da mass shift. Accurate determination of protein glycosylation sites by the current method of identification of deamidated Asn within the consensus sequence Asn-X-Ser/Thr is hindered as deamidation of Asn residues occurs both enzymatically and chemically, resulting in false positives. Chemical deamidation is a pH dependent process that results in the formation of both n-Asp and i-Asp, which can be chromatically resolved. Whereas enzymatic deamidation as seen in PNGase F deglycosylation, results in a one peak from the conversion of the glycosylation Asn residue into n-Asp. By utilizing the NIFP method, N-linked glycosylation sites can be identified by the presence of an n-Asp residue, not a mixture of n- and i-Asp, within the consensus sequence Asn-X-Ser/Thr. The site is considered to be deamidated if the chromatogram shows the presence of peaks corresponding to the n-Asp and i-Asp. The intent of this study is to alert investigators in the field

to the potential and unexpected errors resulting from this phenomenon and to suggest strategies to overcome this pitfall and prevent the identification of false positives.

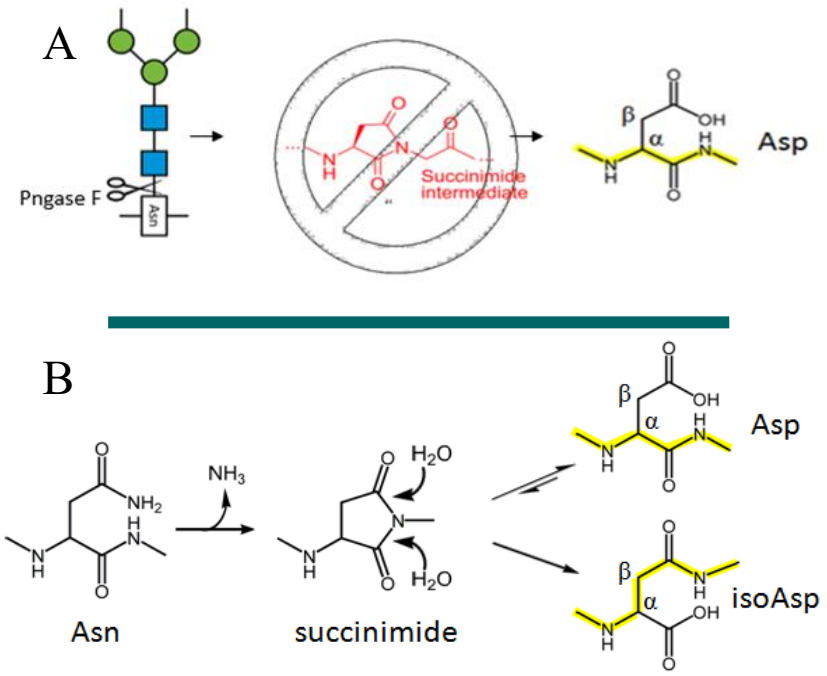

Figure 1. A) Mechanism of PNGase F deglycosylation B) Mechanism of Asn Deamidation and Asp Isomerization via a Succinimide Intermediate. The peptide backbone is highlighted in yellow.

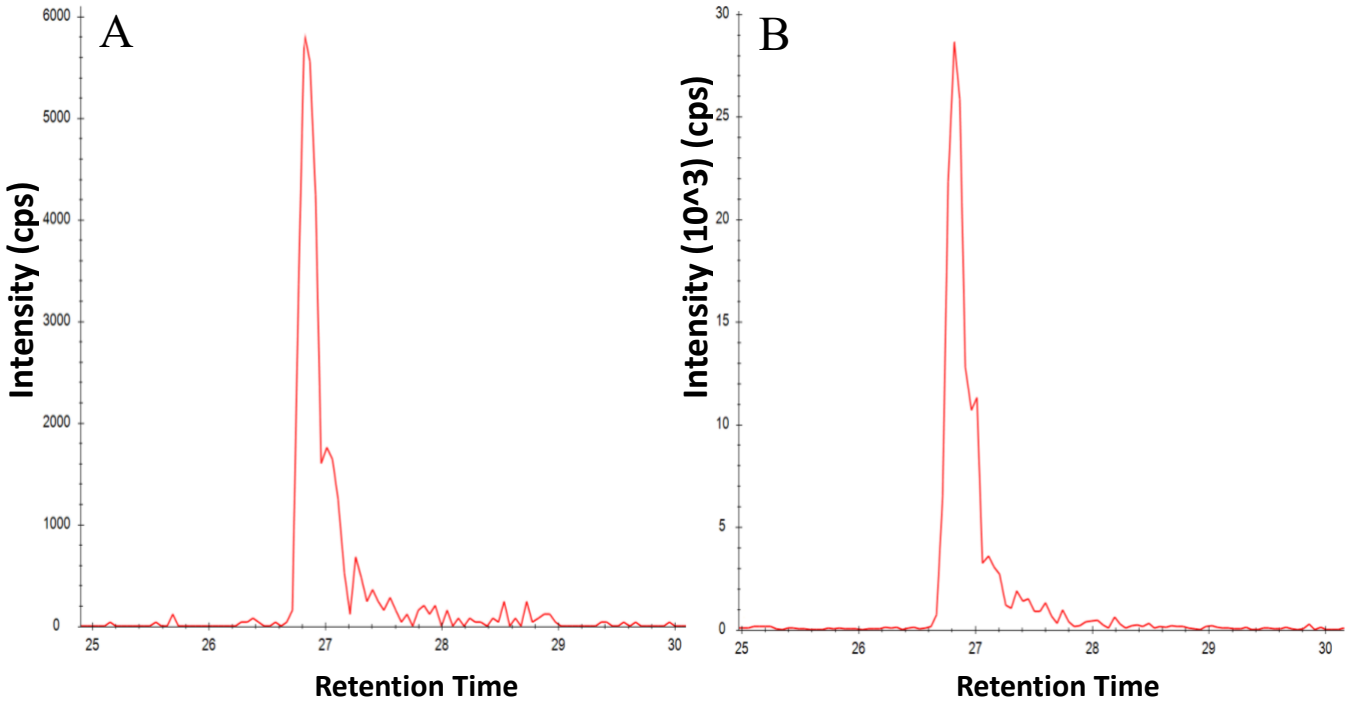

Figure 2. The selected reaction monitoring chromatogram of the IgG glycosylated peptide EEQYNSTYR with glycan A2G0F attached ($[1317.53]^{++}$) incubating at A) pH 6.8 (left) and B) pH 7.8 (right) at 37 °C for 48 hours.

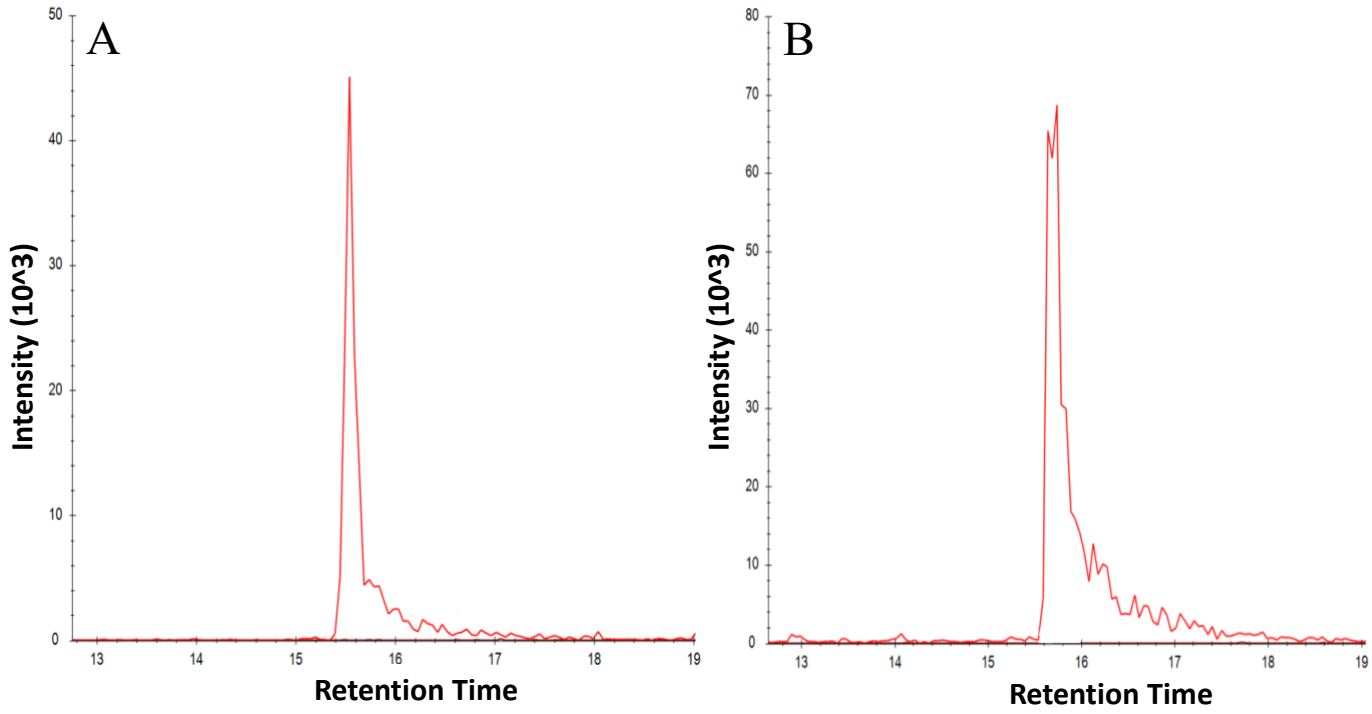

Figure 3. The selected reaction monitoring chromatogram of the IgG glycosylated peptide EEQYNSTYR ($[1189.51]^{+}$) after treatment with PNGase F incubating at A) pH 6.8 (left) and B) pH 7.8 (right) at 37 °C for 96 hours total.

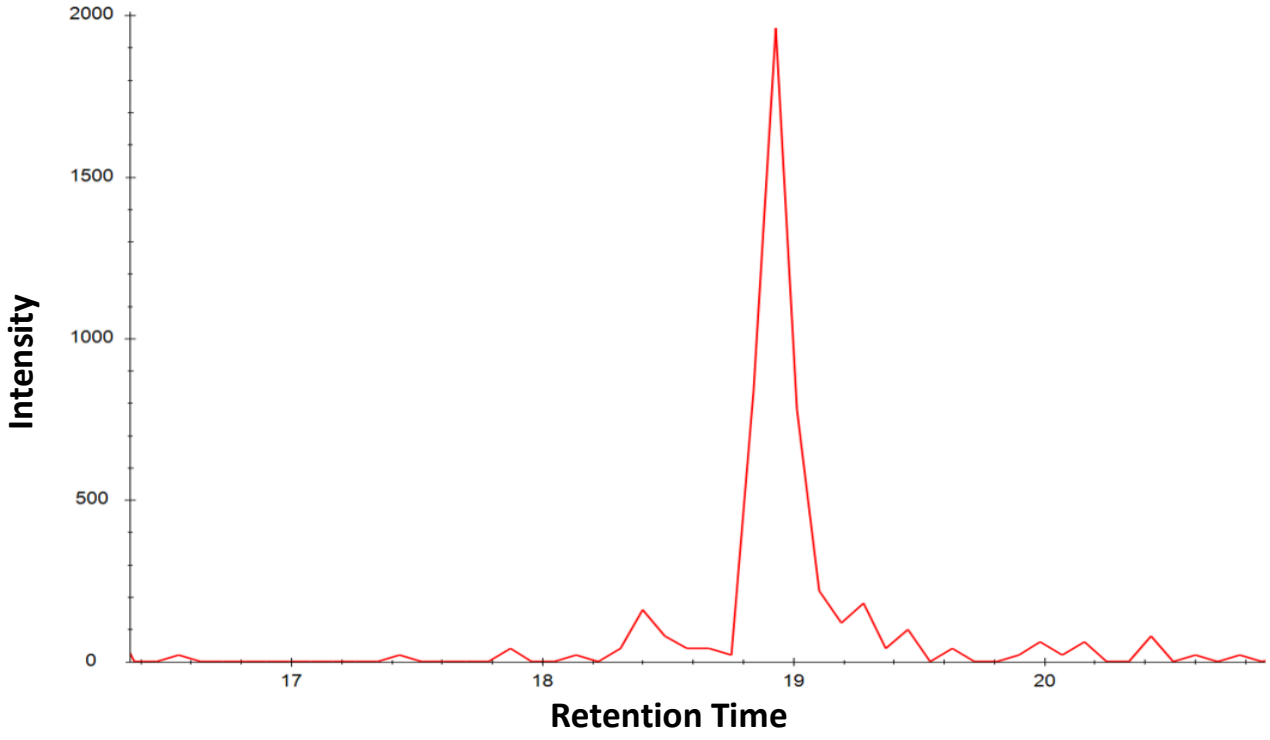

Figure 4. The selected reaction monitoring chromatogram of the HER2 glycosylated peptide GHCWGPGPTQCVNCSQFLR ($[1130.99]^{++}$ incubating at 37°C at pH 7.8 for 96 hours after deglycosylation with PNGase F.

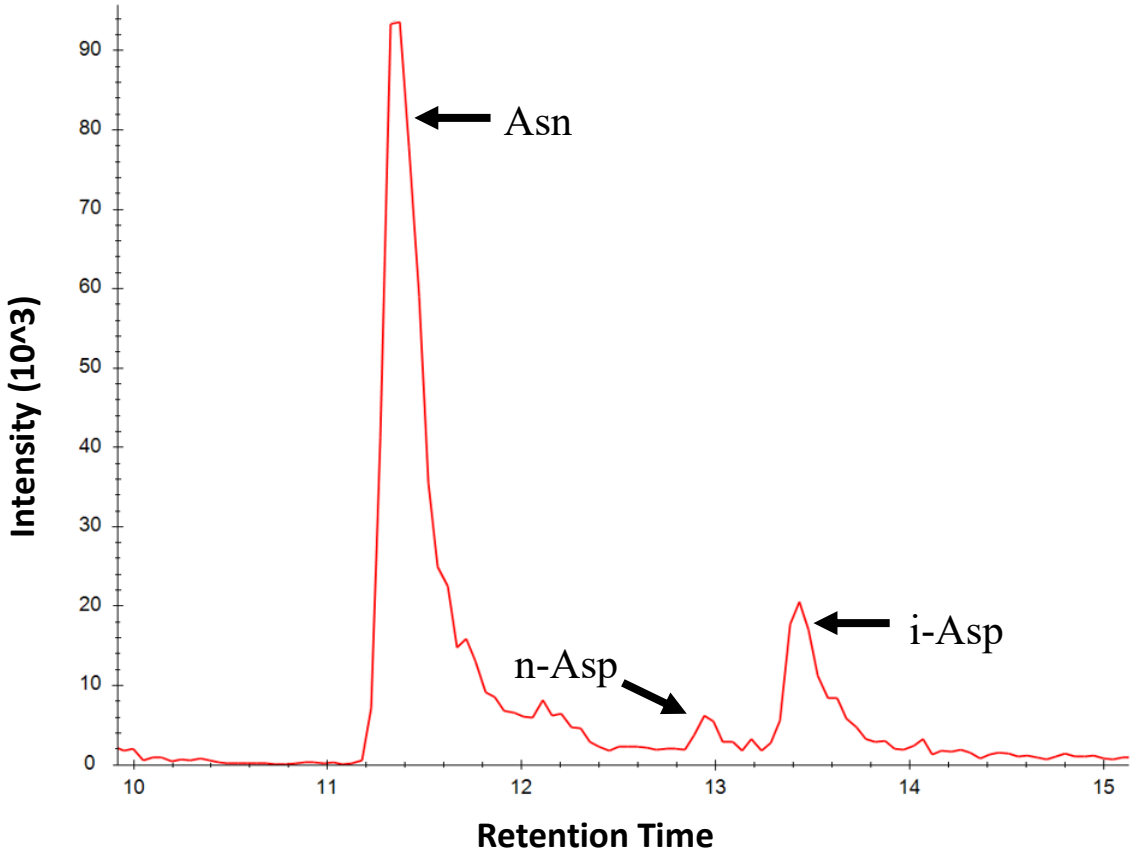

Figure 5. The selected reaction monitoring chromatogram of the IgG deamidated peptide VVSVLTVLHQDWLNGK ($[904.51]^{+}$) incubating at pH 7.8 and 37 °C for A) 48 hours and B) 96 hours and PNGase F deglycosylation. Illustrates how we can separate the n-Asp, and i-Asp versions. In Figure 5A, the peak at 11.4 minutes represents amidated Asn, which is also the most prominent peak in the chromatogram. The peak at 12.9 minutes represents n-Asp and the peak at 13.4 minutes represents i-Asp, highlighted by. The i-Asp is three times the size as n-Asp.

CHAPTER 5

SOLVING THE AGE-OLD QUESTION: DO I NEED TO TRYPSIN DIGEST BEFORE RELEASING IGG GLYCANS WITH PNGASE-F

Birx, L., Popov, M., Orlando, R. To be submitted to *Journal of Biomolecular Techniques.*

Abstract

Immunoglobulin G (IgG) is the main immunoglobulin in human serum, and its biological activity is modulated by glycosylation on its fragment crystallizable region (Fc). Glycosylation of IgGs has shown to be related to aging, disease progression, protein stability, and many other vital processes. A common approach to analyze IgG glycosylation involves the release of the N-glycans by PNGase F, which cleaves the linkage between the asparagine (Asn) residue and the innermost N-acetylglucosamine (GlcNAc) of all N-glycans except those containing a 3-linked fucose attached to the core GlcNAc. The biological significance of these glycans makes the development of accurate and fast methods that provide a complete glycan release is vital. Currently, researchers either perform PNGase F deglycosylation on intact or trypsin digested IgGs. Those who perform PNGase F deglycosylation on trypsin digested IgGs argue that proteolysis is needed to reduce steric hindrance while the other states that this step is not needed. There is minimal experimental evidence supporting either assumption. The importance of obtaining complete glycan release for accurate quantitation led us to investigate the kinetics of this deglycosylation reaction for intact IgGs and IgG glycopeptides and to determine the effect of trypsin digestion on the rate of glycan release from glycopeptides of IgGs. Statistically significant differences in the rate of deglycosylation performed on intact IgGs and trypsin digested IgGs was determined and the rate of PNGase F deglycosylation on trypsin digested IgGs was found to be 3-4 times faster than on intact IgG.

Introduction

Immunoglobulin G (IgG) is the most abundant antibody in the human body, made up of two heavy chains and two light chains. IgGs are involved in multiple humoral immune processes including antigen neutralization, complement activation and complement dependent cytotoxicity

(CDC), and antibody-dependent cell-mediated cytotoxicity (ADCC).[81] There are four subclasses of IgGs (IgG1, IgG2, IgG3, and IgG4), that differ in their constant regions, particularly in their hinges and upper CH2 domains.[4] All IgGs are N-glycosylated at aspargine-297 (Asn-297) in the CH_2 domain of the crystallizable fragment (Fc) part of the heavy chains. In human IgG, the majority of the Fc glycans are complex biantennary structures with a high degree of heterogeneity, due to the presence or absence of different terminal sugars. IgG glycosylation has been shown to be related to aging, analyzed for disease diagnosis and progression.[82] The biological significance of these glycans makes the development of accurate methods to analyze them vital.

N-linked glycosylation follows a conserved consensus sequence of Asn-X-Serine/Threonine, where X is any amino acid except proline.[75] Peptide-N4-(N-acetyl-beta-glucosaminyl)asparagine amidase (PNGase F) is commonly used to remove N-linked glycans. PNGase F cleaves the glycosidic bond between the carbohydrate-holding Asn residue, converts the Asn residue to aspartic acid and releases ammonia and the intact glycan, while generating a carbohydrate-free peptide.[137,134] PNGase F is not able to cleave N-linked glycans from glycoproteins when the innermost GlcNAc residue is linked to an α1-3 Fucose residue. This modification is most commonly found in plant and some insect glycoproteins.[138,139]

Analysis of IgG glycosylation is typically done by releasing the N-glycans using PNGase-F. Complete release of all glycans is necessary for accurate quantitation. There is a current divide on the benefits of trypsin digestion prior to PNGase-F release. One camp argues that proteolysis is needed to reduce steric hindrance while the other states that this step is not needed. There is minimal experimental evidence supporting either assumption. The importance of obtaining complete glycan release for accurate quantitation led us to investigate the kinetics of

this deglycosylation reaction for intact IgGs and IgG glycopeptides and to determine the effect of trypsin digestion on the rate of glycan release from glycopeptides of IgGs. Studies have shown that trypsin digestions on glycoproteins have a possibility of being incomplete due to glycan steric hindrance[140,141] but until now, no study has investigated the effect of steric hindrance on deglycosylation kinetics.

To facilitate the analysis of IgG glycosylation, we are investigating the kinetics of PNGase-F deglycosylation on both intact and trypsin digested IgGs to determine the effect of trypsin digestion on the rate of glycan release from IgG-glycopeptides. It is hypothesized that the rate of PNGase-F deglycosylation will be faster on the sample treated with trypsin beforehand.

Methods

The overall experimental workflow is shown in Fig. 1.

Human serum, trypsin (tosyl phenyl alanyl chloromethyl ketone (TPCK) treated), dithiothreitol (DTT), iodoacetamide (IDA), ammonium bicarbonate, ammonium formate, and formic acid (liquid chromatography (LC) – mass spectrometry (MS) grade) were purchased from Sigma-Aldrich (St. Louis, MO, USA). Acetonitrile (ACN; LC-MS grade) was purchased from Thermo Fisher Scientific (Waltham, MA, USA). Other reagents were analytical grade.

A Hi-Trap™ protein G column (Cytiva, Uppsala, Sweden) was used to purify IgGs from Human Serum (HSPD IgGs). An initial solution containing intact HS-IgGs in 50 mM ammonium bicarbonate (pH 7.8) was spiked with [Glu1]-Fibrinopeptide B (quantitation standard) (GluFib) and trypsin digested SILAC labeled IgG1 (kinetic standard) (GlycoScientific, Athens, GA). This solution was split in half, one half was digested with trypsin first and the other was deglycosylated with PNGase F first.

For the trypsin first sample, reduction and alkylation were performed with DTT and IDA. The sample was dried to volatilize excess DTT, and IDA remaining and resuspended in 50 mM ammonium bicarbonate (pH 7.8). Next trypsin was added to the sample with the ratio of 1 part trypsin to 20 parts sample, digestion was carried out at 37°C overnight. The trypsin digest sample was dried as means to desalt the sample. The dried tryptic digest was redissolved in 50 mM ammonium bicarbonate. The dissolved tryptic peptides/glycopeptides were then treated with 0.1 U of PNGase F per μg of IgG. Aliquots of the digestion mixture were removed at various time points, quenched by lowering the pH to 3.5 with formic acid, then immediately frozen in dry ice. The samples were dried, then resuspended in 68% ACN for analysis. The ratio of PNGase-F in units to substrate has been experimentally determined so that the deglycosylation reaction takes one hour, which is long enough to allow for sufficient time points to be sampled in a reasonable time period.

Alternatively, the other half of the initial solution containing intact HSPD IgGs was deglycosylated first by treating the sample with 0.1 U of PNGase F per μg of IgG. Aliquots were removed at various time points, quenched by lowering the pH to 3.5 with formic acid, then immediately frozen in dry ice. The aliquots were dried, then resuspended in 50 mM ammonium bicarbonate (pH 7.8) for trypsin digestion. Reduction and alkylation were performed with DTT and IDA on the solubilized intact, deglycosylated IgGs. The sample was dried to volatilize excess DTT, and IDA remaining and resuspended in 50 mM ammonium bicarbonate (pH 7.8). Next trypsin was added to the sample with the ratio of 1 part trypsin to 20 parts sample, digestion was carried out at 37°C overnight. The PNGase F first sample was dried as means to desalt the sample, then resuspended in 68% ACN for analysis. Each reaction was done in four replicates.

LC-MS analysis was performed on a Waters Synapt-G2 with a HP1100 LC. Peptides were separated using a column 2.1 mm x 150- mm HALO ® Penta-HILIC column packed with 2.7 um diameter superficially porous particles that have a 90 Å pore diameter (Advanced Materials Technology, Wilmington, DE, USA) at 60°C. The mobile phases used in the separation were 0.1% formic acid, 50 mM ammonium formate in water (A) and 0.1% formic acid in acetonitrile (B). The glycopeptides were bound to the column in 68% B and a linear gradient to 54% B over 20 minutes was initiated to elute the peptides. Skyline was used for data analysis.[110]

Results & Conclusions

The kinetics of PNGase F deglycosylation reaction were studied by its addition to two solutions, one containing tryptic digested IgG glycopeptides purified human serum and the other solution containing intact IgG purified from human serum. The release of glycans by PNGase F was monitored in both solutions. This approach allowed a broad range of human serum IgG glycopeptides to be monitored simultaneously by LC-MS. The glycan structures of the glycopeptides observed in the human serum IgGs and their abbreviations are shown in Figure 2. The LC-MS chromatograms illustrate how the peak area of the glycopeptides decrease with increasing digestion times (Fig.3). The integrated peak area of each glycopeptide ([GP]) was calculated by dividing the peak area of each glycopeptide by the peak area of the internal standard (GluFib) at each time point.

PNGase F releases N-linked glycans from the peptide backbone by hydrolyzing the amide group of the Asn sidechain (Eq. 1). PNGase F, an enzyme, is neither consumed nor produced during the reaction, thus its concentration stays constant. The concentration of H_2O is in excess compared to the other two reactants and remains constant throughout the process.

Consequently, this third order reaction is a pseudo first-order reaction (Eq. 2), as two of the three reactants are not consumed in the reaction. The differential rate equation describing the decrease in glycopeptide concentration as a function of time for pseudo first-order kinetics is shown in Eq. 3, and the integrated form in Eq. 4. In Eqs. 3 and 4, k is the rate constant.[142]

$$Glycopeptide + H_2O + PNGase\ F \rightarrow N-Glycan + Peptide + PNGase\ F \quad (1)$$

$$Glycopeptide \rightarrow N-Glycan + Peptide \quad (2)$$

$$\frac{-d[GP]}{dt} = k[GP] \quad (3)$$

$$\ln[GP] = -kt + \ln[GP_0] \quad (4)$$

The plotting of the natural log of [GP] (ln [GP]) with respect to time yields a straight line, these plots are referred to as kinetic profiles. The linearity observed confirms that the PNGase F deglycosylation reaction can be modeled as a pseudo first-order process and allows a rate constant for the deglycosylation of each glycopeptide to be determined by calculating the slope of ln [GP] vs. time plots. Figure 4 shows the kinetic profile for IgG1 glycopeptides carrying the Fucosylated glycan with 1 galactose (A2G1F) and the Fucosylated glycan with 2 galactoses (A2G2F) on trypsin digested IgG and on intact IgG. A rate standard of trypsin digested SILAC labeled IgG1 was used to normalize the deglycosylation rate between the samples.

The effects of trypsin digestion on the kinetics of PNGase F deglycosylation were investigated. The slopes of the lines (ln [GP] vs. time), (Fig. 4) which are proportional to the rate constant of the PNGase F release, were calculated for each species and these values are presented in Table 1. For each glycoform, the rate of PNGase F deglycosylation on trypsin digested IgG glycopeptides is 3-4 times faster than on intact IgG. The faster rate of deglycosylation on trypsin

digested IgGs is due to the reduced steric hindrance of the glycopeptides compared to the intact IgGs. The trypsin digest results in glycans that are more accessible to PNGase F allowing for a faster deglycosylation, compared to the glycans being buried in the intact structure.

In this study, the amount of PNGase F used is less than the normal amount done in a lab setting. This was done to slow down the reaction to allow for multiple time points to be collected. To better simulate normal conditions, where more PNGase F is used per μg of glycoprotein, the rate of deglycosylation for each glycoform was multiplied by 100 for the half-life and time until full deglycosylation calculations. Since in this study, 0.1 U PNGase F per μg glycoprotein while the standard amount of PNGase F typically used in a lab setting is 10 U PNGase F per μg glycoprotein. The half-life ($t_{1/2}$) (Eq. 5) of the PNGase F deglycosylation performed on both intact IgGs and trypsin digested IgGs was calculated using this adjusted rate, shown in Table 2. For each glycoform, the half-life of trypsin digested IgG glycopeptides were calculated to be an average of 3 times faster than PNGase F deglycosylation performed on intact IgG. PNGase F deglycosylation performed on trypsin digested IgG has a lower half-life time than PNGase F deglycosylation performed on intact IgG, meaning that it takes less time for the glycopeptides to reach half the initial concentration.

$$t_{1/2} = \frac{\ln 2}{k} \approx \frac{0.693}{k} \quad (5)$$

The time until full deglycosylation can be calculated in multiples of $t_{1/2}$, and after 7 iterations, <0.01% of the glycopeptide would remain, thus this the time until full deglycosylation, shown in Table 2. For PNGase F deglycosylation performed on both trypsin digested IgGs and intact IgGs, the time until full deglycosylation varies depending on the

glycoform. For PNGase F deglycosylation performed on trypsin digested IgGs, the average time until full deglycosylation is 3.12 minutes, but all glycoforms are not fully deglycosylated until 7.3 minutes, when a normal amount of PNGase F is used. For PNGase F deglycosylation performed on intact IgGs, the average time until full deglycosylation is 9.51 minutes, but all glycoforms are not fully deglycosylated until 43.91 minutes, when a normal amount of PNGase F is used. This data suggests that researchers who try to complete a rapid PNGase F glycan release in under 5 minutes, even on trypsin digested IgGs and utilizing a normal amount of PNGase F, may encounter issues with complete deglycosylation, as some glycoforms have not reached full deglycosylation in that time frame.

A Mann-Whitney U test was used to investigate if the differences in rates among deglycosylation performed on tryptic digested IgGs and intact IgGs are statistically significant. The Mann-Whitney U test is a nonparametric test of the null hypothesis, where 2 samples have equal averages, vs. the alternative hypothesis, where the sample means from the 2-samples are not equal. Mann-Whitney U test was selected over the 2-sample t test, as the Mann-Whitney U test does not require the assumption of normal distributions or a specific sample size.[143] The results from this Mann-Whitney U test are listed in Table 3 for each comparison category. The smaller the P value, the more likely one can reject the null hypothesis that the difference between the 2 groups is a result of random sampling. Therefore, small P values lead one to conclude that the populations are distinct. For example, a P value of 0.05 indicates a 5% risk of finding that a difference exists between 2 populations when there is no actual difference.

The results from the rate of deglycosylation performed on every glycoform attached to the intact IgG1 was compared to the rate of deglycosylation performed on every glycoform attached to the IgG1 tryptic glycopeptides. The P value of <0.001 obtained when the rate of

deglycosylation of intact IgGs is compared with the rate of deglycosylation performed on tryptic digested IgG glycopeptides suggests that the observed differences in rate constants between these two groups have a <0.1% chance of arising from random sampling, thus the results are statistically significant.

Conclusion

Significant differences in PNGase F deglycosylation rate constants were observed between IgGs treated with trypsin and intact IgGs. The rate of PNGase F deglycosylation on trypsin digested IgG glycopeptides is 3-4 times faster than on intact IgG. The time until full deglycosylation was also found to be 3-4 times faster on trypsin digested IgGs than on intact IgG. The use of a normal amount of PNGase F would digest intact IgG, just at a slower rate. This data suggests that researchers who try to complete a rapid PNGase F glycan release in under 5 minutes may encounter issues with complete deglycosylation. The differences in deglycosylation rate performed on trypsin digested IgGs and intact IgGs suggest that deglycosylation should be performed on IgGs digested with trypsin to ensure complete deglycosylation in the fastest time to avoid quantitation errors.

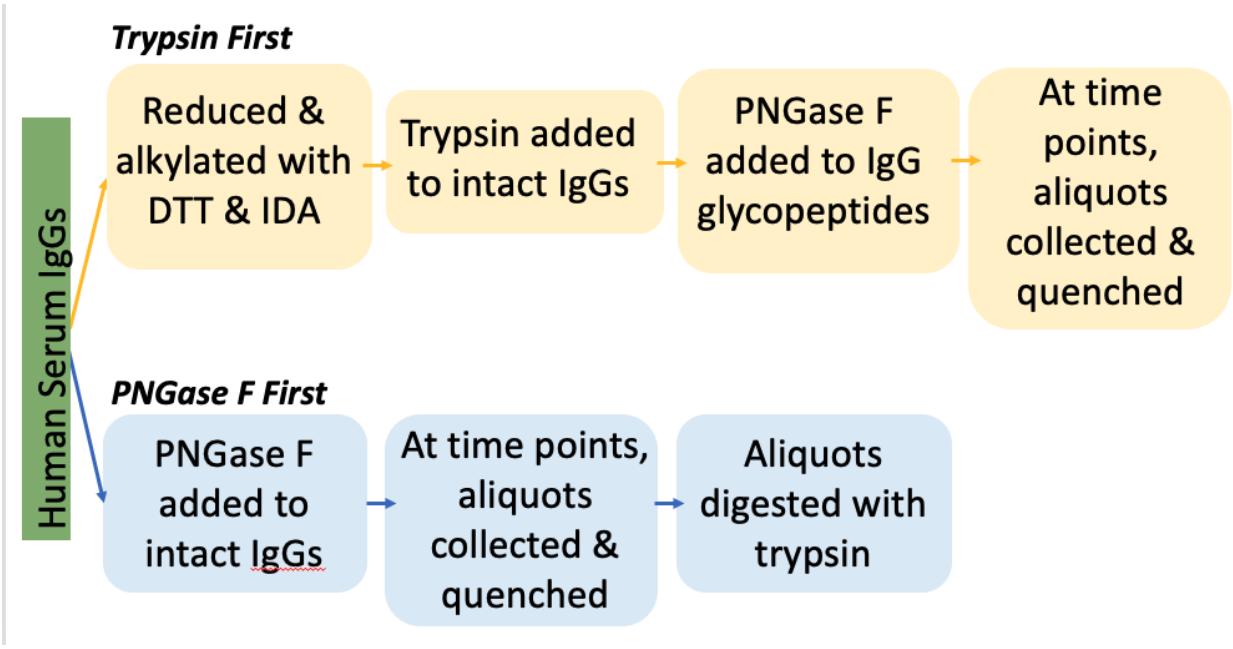

Figure 1. Experimental Workflow.

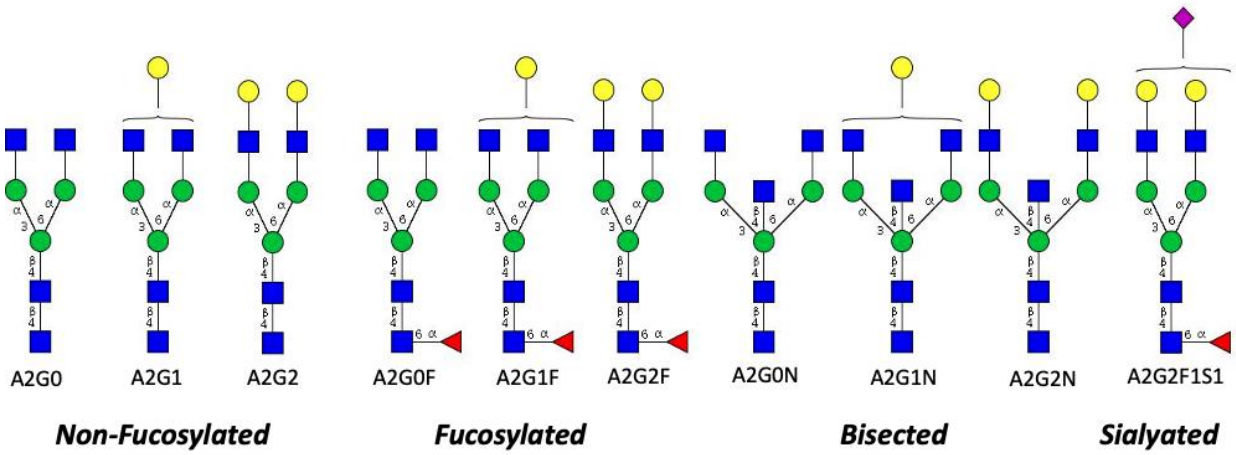

Figure 2. Glycan structures analyzed. Each structure with a “G1” can have two possible linkages of Gal.

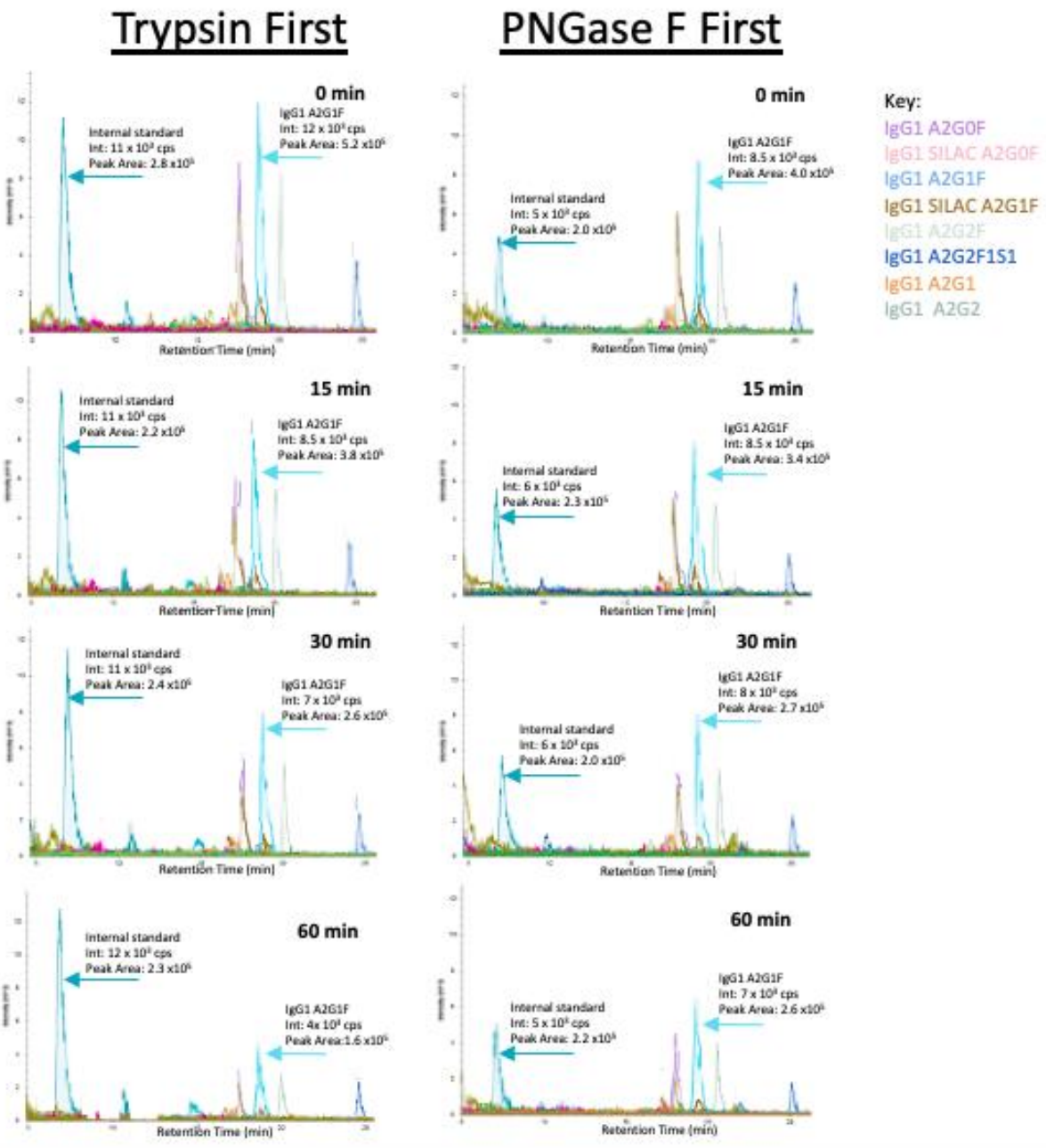

Figure 3. LC-MS Chromatograms show the disappearance of glycopeptide from 0 min to 1 hour for deglycosylation performed on intact and tryptic digested IgGs.

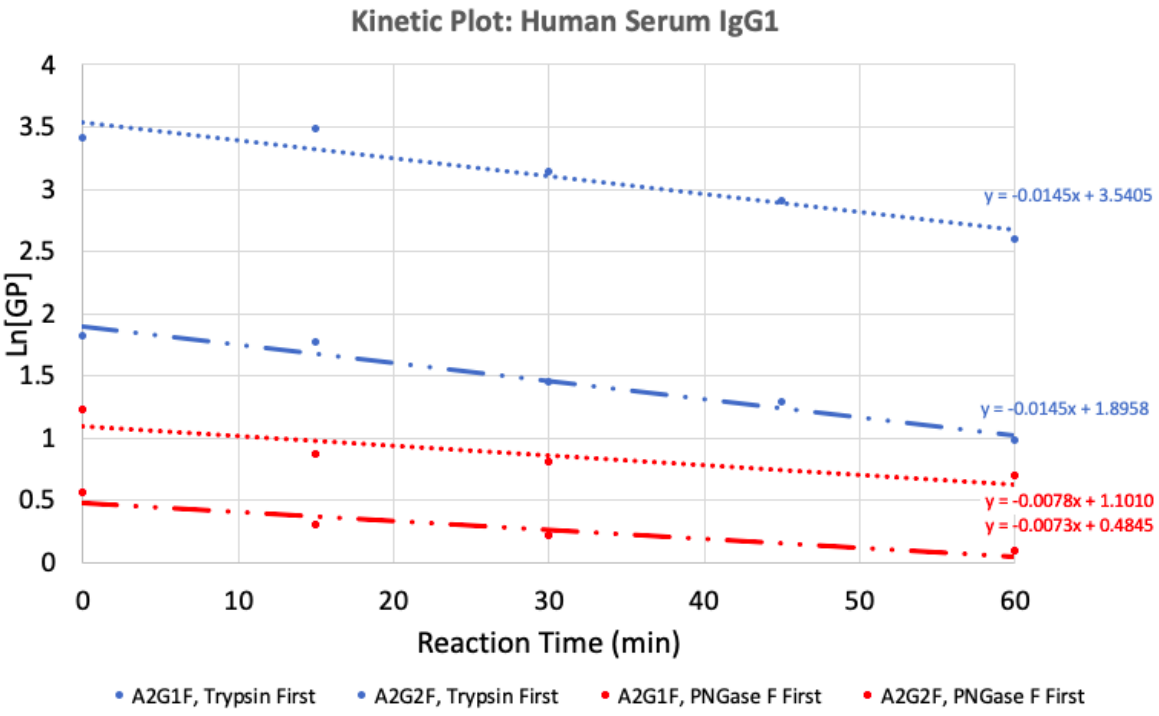

Figure 4. The plot of ln [GP] vs. time for the IgG1 glycopeptide carrying the fucosylated glycan with 1 galactose (A2G1F) and the fucosylated glycan with 2 galactoses (A2G2F). This data was obtained following the addition of PNGase F at a concentration of 0.1 U PNGase F/µg IgG. The kinetic profile for A2G1Fand A2G2F on trypsin digested IgG and on intact IgG is included in the graph.

Table 1. Average Rate of Deglycosylation on Intact Human Serum IgGs and Trypsin Digested Human Serum IgG Glycopeptides.		
	Rate (k) (Average +/- Standard Deviation (SD))	
Glycopeptide	Trypsin digested IgG	Intact IgG
IgG1 A2G0	0.0133 +/- 0.0047	0.0036 +/- 0.0008
IgG1 A2G1	0.0161 +/- 0.0034	0.0082 +/- 0.0013
IgG1 A2G2	0.0139 +/- 0.0054	0.0047 +/- 0.0040
IgG1 A2G0N	0.0297 +/- 0.0042	0.0077 +/- 0.0048
IgG1 A2G1N	0.0263 +/- 0.0047	0.0160 +/- 0.0114
IgG1 A2G2N	0.0293 +/- 0.0104	0.0142 +/- 0.0020
IgG1 A2G0F	0.0171+/- 0.0026	0.0068+/- 0.0028
IgG1 A2G1F	0.0169 +/- 0.0040	0.0070 +/- 0.0036
IgG1 A2G2F	0.0150 +/- 0.0051	0.0066 +/- 0.0027
IgG1 A2G2F1S1	0.0071 +/- 0.0018	0.0045 +/- 0.0032
IgG2/3 A2G2	0.0196 +/- 0.0045	0.0043 +/- 0.0023
IgG2/3 A2G0N	0.0165 +/- 0.0072	0.0058 +/- 0.0056
IgG2/3 A2G1N	0.0150 +/- 0.0053	0.0060 +/- 0.0024
IgG2/3 A2G2N	0.0143 +/- 0.0027	0.0046 +/- 0.0036
IgG2/3 A2G0F	0.0158 +/- 0.0043	0.0048 +/- 0.0042
IgG2/3 A2G1F	0.0181 +/- 0.0056	0.0072 +/- 0.0055
IgG2/3 A2G2F	0.0184 +/- 0.0039	0.0064 +/- 0.0017
IgG2/3 A2G2F1S1	0.0109 +/- 0.0055	0.0023 +/- 0.0019
IgG4 A2G1	0.0178 +/- 0.0046	0.0052 +/- 0.0018
IgG4 A2G2	0.0170 +/- 0.0030	0.0046 +/- 0.0004
IgG4 A2G1N	0.0157 +/- 0.0069	0.0086 +/- 0.0029
IgG4 A2G0F	0.0215 +/- 0.0086	0.0062 +/- 0.0041
IgG4 A2G1F	0.0179 +/- 0.0051	0.0068 +/- 0.0037
IgG4 A2G1NF	0.0101 +/- 0.0042	0.0036 +/- 0.0015

Table 2. Half-life and Time Until Full Deglycosylation on Intact Human Serum IgGs and Trypsin Digested Human Serum IgG Glycopeptides				
	Half-life (min)		Time until Full Deglycosylation (min)	
Glycopeptide	Trypsin digested IgG	Intact IgG	Trypsin digested IgG	Intact IgG
IgG1 A2G0	0.4631	1.6047	3.2416	11.2326
IgG1 A2G1	0.3898	0.8023	2.7288	5.6163
IgG1 A2G2	0.6765	1.6829	4.7353	11.7805
IgG1 A2G0N	0.2184	1.0952	1.5285	7.6667
IgG1 A2G1N	0.2760	0.5610	1.9320	3.9268
IgG1 A2G2N	0.2240	0.5111	1.5682	3.5778
IgG1 A2G0F	0.3485	0.9079	2.4394	6.3553
IgG1 A2G1F	0.4083	0.8846	2.8580	6.1923
IgG1 A2G2F	0.4759	0.9452	3.3310	6.6164
IgG1 A2G2F1S1	1.0299	1.6047	7.2090	11.2326
IgG2/3 A2G2	0.3382	1.9167	2.3676	13.4167
IgG2/3 A2G0N	0.4083	1.4681	2.8580	10.2766
IgG2/3 A2G1N	0.4083	1.3019	2.8580	9.1132
IgG2/3 A2G2N	0.7931	1.3019	5.5517	9.1132
IgG2/3 A2G0F	0.4313	1.2321	3.0188	8.6250
IgG2/3 A2G1F	0.3730	0.8625	2.6108	6.0375
IgG2/3 A2G2F	0.3467	1.4681	2.4271	10.2766
IgG2/3 A2G2F1S1	0.6106	6.2727	4.2743	43.9091
IgG4 A2G1	0.3270	0.7753	2.2891	5.4270
IgG4 A2G2	0.4792	1.1897	3.3542	8.3276
IgG4 A2G1N	0.4286	0.7753	3.0000	5.4270
IgG4 A2G0F	0.2936	1.0781	2.0553	7.5469
IgG4 A2G1F	0.3382	1.0615	2.3676	7.4308
IgG4 A2G1NF	0.6000	1.3019	4.2000	9.1132

Table 3. Results of Mann-Whitney Test: Calculating the Significance of Differences in Rates Among Deglycosylation Performed on Tryptic Digested IgGs and Intact IgGs		
Comparison	**P**	**Result**
k (IgG1 - trypsin first) vs. k (IgG1 - PNGase F first)	<0.001	k (IgG1 - PNGase F first) < k (IgG1 - trypsin first)
k (IgG2/3 - trypsin first) vs. k (IgG2/3 - PNGase F first)	<0.001	k (IgG2/3 - PNGase F first) < k (IgG2/3 - trypsin first)
k (IgG4 - trypsin first) vs. k (IgG4 - PNGase F first)	<0.001	k (IgG4 - PNGase F first) < k (IgG4 - trypsin first)

CHAPTER 6

ARE ALL PNGASE F'S CREATED EQUALLY? INVESTIGATING THE KINETICS OF DEGLYCOSYLATING HUMAN SERUM IGGS WITH DIFFERENT ENZYME PREPARATOINS

Birx, L., Orlando, R. To be submitted to *Journal of Biomolecular Techniques.*

Abstract

The glycosylation of IgGs has a significant role in its biological activity and the pathophysiology of many different diseases. A common approach to analyze IgG glycosylation involves the release of the N-glycans by Peptide-N4-(N-acetyl-beta-glucosaminyl)asparagine amidase (PNGase F), which cleaves the linkage between the asparagine (Asn) residue and the innermost N-acetylglucosamine (GlcNAc) of all N-glycans except those containing a 3-linked fucose attached to the core GlcNAc. The importance of obtaining complete glycan release for accurate quantitation led us to investigate the kinetics of PNGase F deglycosylation reaction for multiple preps, where three PNGase F enzyme preparations were compared (one amidase and two recombinant versions). Statistically significant differences in the rate of deglycosylation performed using three different PNGase F enzyme preps on trypsin digested IgGs was determined and the rate of PNGase F deglycosylation with prep 3 deglycosylated IgG tryptic glycopeptides at a rate 34 times faster than prep 1, and PNGase F prep 1 deglycosylated IgG tryptic glycopeptides at a rate 5 times faster than prep 2.

Introduction

Immunoglobulin G (IgG), a serum glycoprotein, is the most abundant antibody in the human body. IgGs are involved in multiple human humoral immune processes including antigen neutralization, complement activation and complement dependent cytotoxicity (CDC), and antibody-dependent cell-mediated cytotoxicity (ADCC).[81] There are four subclasses of IgGs (IgG1, IgG2, IgG3, and IgG4), that differ in their constant regions, particularly in their hinges and upper CH2 domains.[4] Immunoglobulin G1 (IgG1) is the most abundant IgG, followed by IgG2, IgG3, and IgG4 being the least abundant. All IgGs are N-glycosylated at aspargine-297 (Asn-297) in the CH_2 domain of the crystallizable fragment (Fc) part of the heavy chains. In

human IgG, the majority of the Fc glycans are complex biantennary structures with a high degree of heterogeneity, due to the presence or absence of different terminal sugars. The glycans attached can affect protein stability, bioactivity, and immunogenicity.[82,74] The biological significance of these glycans makes the development of accurate methods to analyze them vital.

Peptide-N4-(N-acetyl-beta-glucosaminyl)asparagine amidase (PNGase F) is commonly used to remove N-linked glycans. PNGase F mechanism cleaves the glycosidic bond between the carbohydrate-holding Asn residue, converts the Asn residue to aspartic acid (Asp) and releases ammonia and the intact glycan, while generating a carbohydrate-free peptide.[137,134] PNGase F is not able to cleave N-linked glycans from glycoproteins when the innermost GlcNAc residue is linked to an α1-3 Fucose residue. This modification is most commonly found in plant and some insect glycoproteins.[138,139]

The broad specificity and ability to deglycosylate a wide range of glycan structures has led PNGase F to be the most widely used enzyme for releasing N-glycans in glycoanalytical workflows. Over the past decade, protocols for the enzymatic release of N-glycans with PNGase F have been investigated to improve the structural profiling of N-glycans. In a typical workflow, PNGase F is added to intact or denatured glycoproteins and the release of N-glycans is performed in solution by incubation at 37 °C for a few hours or overnight. However, despite the long incubation time, this typical workflow can result in an incomplete release of N-glycans.[144] Many attempts have been made to shorten the incubation time while improving the completeness of deglycosylation including the use of microwave reactors and immobilization of PNGase F on monolithic supports.[145,146] Recent research found that performing PNGase F deglycosylation on trypsin digested IgGs was 3-4 times faster than deglycosylation performed on intact IgGs.

In 2017, research done by Huang and Orlando revealed that significant errors in quantitation of IgG glycosylation can occur due to differences in the release kinetics of N-glycans with different structures.[147] These errors can result in inaccurate N-glycan composition profiling and improper glycan site occupancy.[144] The importance of obtaining complete glycan release for accurate quantitation led us to investigate the kinetics of deglycosylating trypsin digested human serum IgGs with three different PNGase F enzyme preparations.

Methods

The overall experimental workflow is shown in Figure 1.

Human serum (HS), trypsin (tosyl phenyl alanyl chloromethyl ketone (TPCK) treated), dithiothreitol (DTT), iodoacetamide (IDA), ammonium bicarbonate, ammonium formate, and formic acid (liquid chromatography (LC) – mass spectrometry (MS) grade) were purchased from Sigma-Aldrich (St. Louis, MO, USA). Acetonitrile (ACN; LC-MS grade) was purchased from Thermo Fisher Scientific (Waltham, MA, USA). All reagents used were analytical grade. Three different PNGase F enzymes preparations were obtained.

A Hi-Trap™ protein G column (Cytiva, Uppsala, Sweden) was used to purify IgGs from Human Serum (HSPD IgGs). An initial solution containing intact HSPD-IgGs in 50 mM ammonium bicarbonate (pH 7.8) was spiked with [Glu1]-Fibrinopeptide B (quantitation standard) (GluFib).

Prior to the trypsin digest, reduction was performed with 200 mM dithiothreitol (DTT) and alkylated using 1M iodoacetamide (IDA), to a final concentration of 5 mM DTT and 8 mM IDA. The sample was dried to volatilize excess DTT and IDA remaining, then resuspended in 50 mM ammonium bicarbonate (pH 7.8). Next trypsin was added to the sample with the ratio of

1 part trypsin to 20 parts sample, digestion was carried out at 37°C overnight. The trypsin digest sample was dried as means to desalt the sample.

For the PNGase F deglycosylation, three preps (preps 1, 2, and 3) were used to investigate the effect of different PNGase F enzyme preparations on the rate of deglycosylation on tryptic digested glycopeptides. For this, the same amount of PNGase F enzyme was used in each prep and the exact same protocol was performed, the only difference was the manufacturer preparation of PNGase F enzyme used. Prior to PNGase F deglycosylation, the dried tryptic digest was redissolved in 50 mM ammonium bicarbonate. The dissolved tryptic peptides/glycopeptides were then treated with 0.1 U of PNGase F per μg of IgG. Aliquots of the digestion mixture were removed at various time points, quenched by lowering the pH to 3.5 with formic acid, then immediately frozen in dry ice. The samples were dried, then resuspended in 68% ACN for analysis. The ratio of PNGase-F in units to substrate has been experimentally determined so that the deglycosylation reaction takes one hour, which is long enough to allow for sufficient time points to be sampled in a reasonable time-period. Each reaction was done in three replicates.

LC-MS analysis was performed on a Waters Synapt-G2 with a HP1100 LC. Peptides were separated using a 2.1 mm x 150 mm HALO ® Penta-HILIC column packed with 2.7 um diameter superficially porous particles that have a 90 Å pore diameter (Advanced Materials Technology, Wilmington, DE, USA) at 60°C. The mobile phases used in the separation were 0.1% formic acid, 50 mM ammonium formate in water (A) and 0.1% formic acid in acetonitrile (B). The glycopeptides were bound to the column in 68% B and a linear gradient to 54% B over 20 minutes was initiated to elute the peptides. Skyline was used for data analysis.[110]

Results & Conclusions

The effect of different PNGase F enzyme preparations on the rate of deglycosylation of tryptic digested IgG glycopeptides were investigated. Three different PNGase F enzyme preparations (preps) were utilized, Prep 1 was an amidase purified from *Flavobacterium meningosepticum*. PNGase F Prep 2 was a recombinant amidase, cloned from *Elizabethkingia miricola* (formerly *Flavobacterium meningosepticum*) and expressed in *E. coli.* Lastly, the PNGase F utilized in Prep 3 was obtained from a local manufacturer, cloned from *Elizabethkingia meningosepticum,* and expressed in *E. coli.* The same amount of PNGase F enzyme in units was added to a constant amount of tryptic digested Human Serum IgGs so the rate of deglycosylation in all three preps could be compared. For each PNGase F prep, the same experimental conditions were performed and GluFib was utilized as an internal standard.

The differences in the kinetics of PNGase F deglycosylation reaction were studied for three PNGase F preps. In all preps, the release of glycans by PNGase F was monitored. This approach allowed a broad range of human serum IgG glycopeptides to be monitored simultaneously by LC-MS. The glycan structures of the glycopeptides observed in the human serum IgGs and their abbreviations are shown in Figure 2. The LC-MS chromatograms illustrate how the peak area of the glycopeptides decrease with increasing digestion times for each PNGase F prep (Fig.3). The integrated peak area of each glycopeptide ([GP]) was calculated by dividing the peak area of each glycopeptide by the peak area of the internal standard (GluFib) at each time point.

PNGase F releases N-linked glycans from the peptide backbone by hydrolyzing the amide group of the Asn sidechain (Eq. 1). In this deglycosylation reaction, the concentration of PNGase F is constant throughout the reaction as it is an enzyme and is neither consumed nor

produced. The concentration of H_2O is also constant throughout the reaction as it is in excess compared to the other two reactants. Thus, this third order reaction is a pseudo first-order reaction (Eq. 2), as two of the three reactants are not consumed. The differential rate equation describing the decrease in glycopeptide concentration as a function of time for pseudo first-order kinetics is shown in Equation 3, and the integrated form in Equation 4. In Equations 3 and 4, k is the rate constant.[142]

$$Glycopeptide + H_2O + PNGase\ F \rightarrow N-Glycan + Peptide + PNGase\ F \quad (1)$$

$$Glycopeptide \rightarrow N-Glycan + Peptide \quad (2)$$

$$\frac{-d[GP]}{dt} = k[GP] \quad (3)$$

$$\ln[GP] = -kt + \ln[GP_0] \quad (4)$$

The slope of the line in the ln [GP] as a function of time plots (ln [GP] vs. time plot) is proportional to the rate constant of the PNGase F release, and were calculated for each species (Table 1). The linearity of the ln [GP] vs. time plot, also referred to as kinetic plots, confirms that the PNGase F deglycosylation reaction follows a pseudo first-order process. The rate of deglycosylation was fastest for PNGase F Prep 3, then PNGase F Prep 1, and PNGase F Prep 2 had the slowest rate of deglycosylation. It was calculated that PNGase F prep 3 deglycosylated trypsin digested IgG glycopeptides at a rate 34 times faster than Prep 1, and that PNGase F Prep 1 deglycosylated IgG tryptic glycopeptides at a rate 5 times faster than Prep 2.

The fast rate of deglycosylation in Prep 3 is highlighted in Figure 3. For Preps 1 and 2 in Figure 3, the chromatogram from 0 minutes shows a ratio of internal standard to IgG1 glycopeptides that is 1:1. While for Prep 3 the ratio is not 1:1, there is more internal standard

present than IgG1 glycopeptide at 0 minutes. This is due to the fast deglycosylation rate of Prep 3, thus substantial deglycosylation has already occurred at the "0-minute time point".

In this study, the amount of PNGase F used is less than the normal amount used in a lab setting. This was done to slow down the reaction to allow for multiple time points to be collected. To better simulate normal conditions, where more PNGase F is used per μg of glycoprotein, the rate of deglycosylation for each glycoform were multiplied by 100 for the half-life and time until full deglycosylation calculations. Since in this study, 0.1 U PNGase F per μg glycoprotein while the standard amount of PNGase F typically used in a lab setting is 10 U PNGase F per μg glycoprotein. The half-life ($t_{1/2}$) (Eq. 5) for the PNGase F deglycosylation reaction of trypsin digested human serum IgGs for the three different PNGase F enzyme preparations was calculated using this adjusted rate, shown in Table 2. For PNGase F Prep 3, the half-life of the IgG glycoforms being deglycosylated were calculated to be an average of 33 times faster than the half-life calculated for PNGase F deglycosylation with Prep 1. PNGase F deglycosylation performed using Prep 3 has a lower half-life time than Preps 1 and 2, meaning that it takes less time for the glycopeptides to reach half their initial concentration, thus the glycopeptides are deglycosylating faster in Prep 3. For PNGase F Prep 1, the half-life of the IgG glycoforms being deglycosylated were calculated to be an average of 5 times faster than the half-life calculated for PNGase F deglycosylation with prep 2. This supports previous findings and indicates that PNGase F deglycosylation performed using Prep 3 is fastest, then Prep 1, and Prep 2 is the slowest.

$$t_{1/2} = \frac{\ln 2}{k} \approx \frac{0.693}{k} \quad (5)$$

The time until full deglycosylation can be calculated in multiples of $t_{1/2}$, and after 7 iterations, <0.01% of the glycopeptide would remain, shown in Table 2, for each Prep. For PNGase F deglycosylation performed utilizing the three Preps, the time until full deglycosylation varies depending on the glycoform. For deglycosylation performed on trypsin digested IgGs with Prep 3 with a normal amount of PNGase F, the average time until full deglycosylation is 0.08 minutes, but all glycoforms are not fully deglycosylated until 0.13 minutes. Prep 1 was calculated to have an average time until full deglycosylation of 2.74 minutes, and the average time until full deglycosylation for Prep 2 was 12.64 minutes. These findings support that the rate of deglycosylation of tryptic digested IgG glycopeptides is fastest with Prep 3.

A higher abundance of sialylated and bisected N-glycan structures were observed for PNGase F deglycosylation Prep 3 compared to Preps 1 and 2. The PNGase F Prep 3 was more efficient at cleaving complex N-glycans compared to Preps 1 and 2.

A Mann-Whitney U test was performed to determine the significance of the rates of deglycosylation on tryptic IgG glycopeptides for each PNGase F Prep, and the results are shown in Table 3. The Mann-Whitney U test is a nonparametric test of the null hypothesis, where 2 samples have equal averages, vs. the alternative hypothesis, where the sample means from the 2-samples are not equal. Mann-Whitney U test was selected over the 2-sample test, as the Mann-Whitney U test does not require the assumption of normal distributions or a specific sample size.[143] The Mann-Whitney U test calculates a P-value that can be used to determine the significance of the results. The smaller the P-value, the more likely one can reject the null hypothesis that the difference between the 2 groups is a result of random sampling. Therefore, small P values lead one to conclude that the populations are distinct. For example, a P-value of 0.05 indicates a 5% risk of finding that a difference exists between 2 populations when there is

no actual difference. The Mann-Whitney U test revealed that the rates of deglycosylation of glycopeptides using PNGase F prep 3 are statistically faster than deglycosylation of glycopeptides by PNGase F prep 1 or PNGase F prep 2. The P-value of <0.001 obtained when the PNGase prep 3 is compared with the PNGase prep 2 suggests that the observed differences in rate constants between these two groups have a <0.1% chance of arising from random sampling. Likewise, when the PNGase F prep 1 was compared to PNGase F prep 2.

Conclusion

Significant differences in deglycosylation rate utilizing different PNGase F Preps were observed on tryptic digested IgGs. The rate of PNGase F deglycosylation on trypsin digested IgG glycopeptides using PNGase F Prep 3 was 34 times faster than the deglycosylation rate from PNGase F Prep 1. Half-life and time until full deglycosylation calculations performed for using the rate of deglycosylation for each Prep, further support findings. The differences in deglycosylation rate of the three Preps performed on trypsin digested IgGs suggest that deglycosylation should be performed with PNGase F Prep 3 to ensure complete deglycosylation in the fastest time to avoid quantitation errors due to incomplete deglycosylation.

Acknowledgements

Authors thank Sean Wu from Lectenz®Bio for the donation of the PNGase F enzyme utilized in Prep 3.

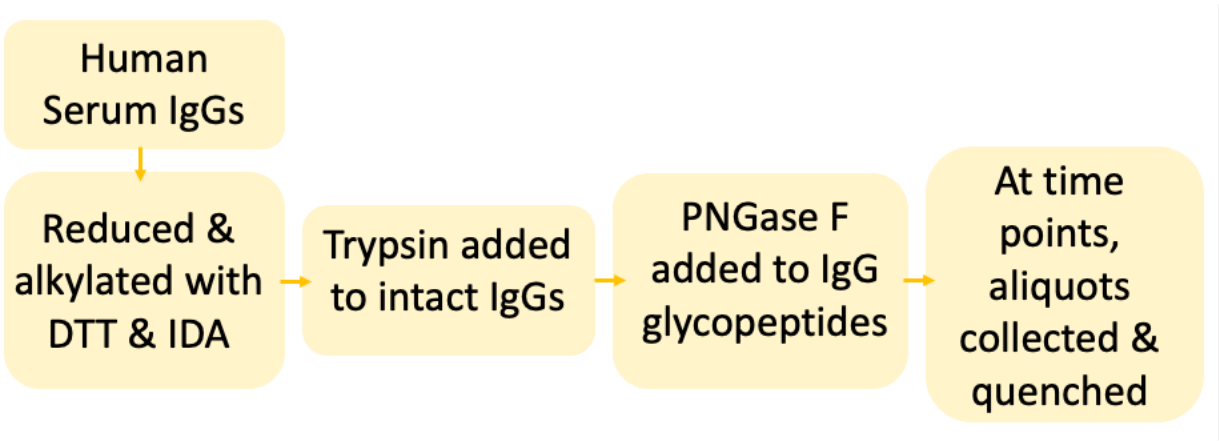

Figure 1. Experimental Workflow.

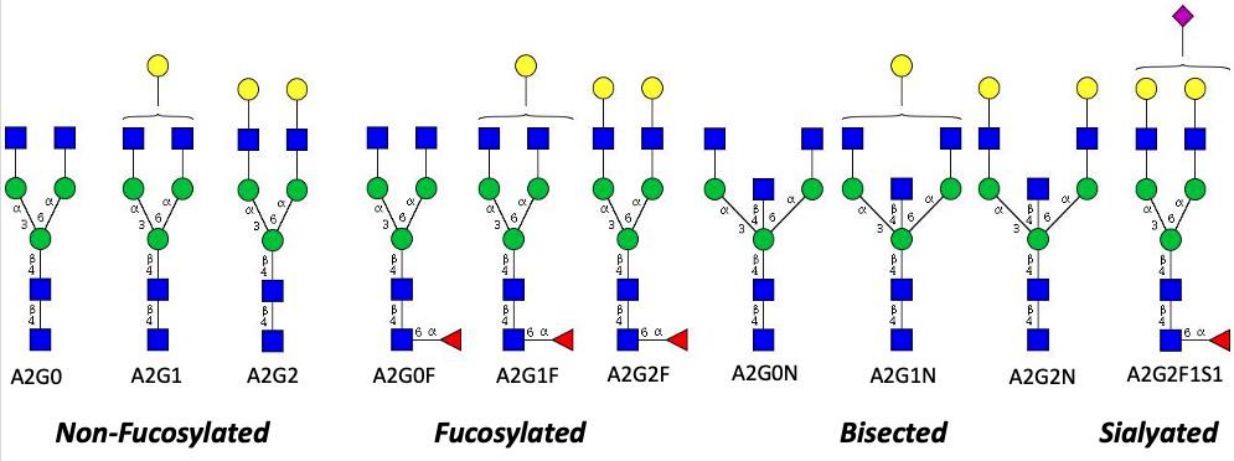

Figure 2. Glycan structures analyzed. Each structure with a “G1” can have two possible linkages of Gal.

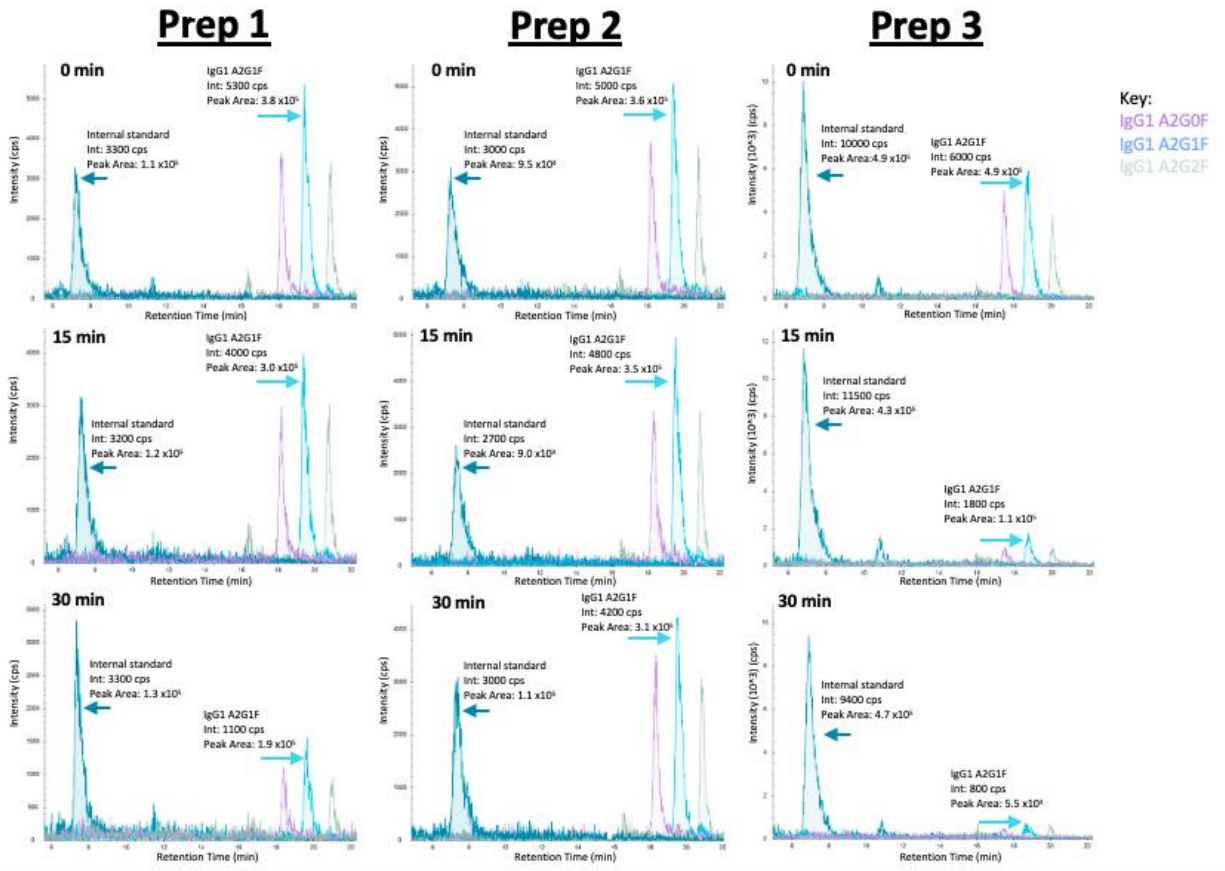

Figure 3. LC-MS Chromatograms show the disappearance of glycopeptide from 0 min to 30 min for deglycosylation performed using the three PNGase F preps.

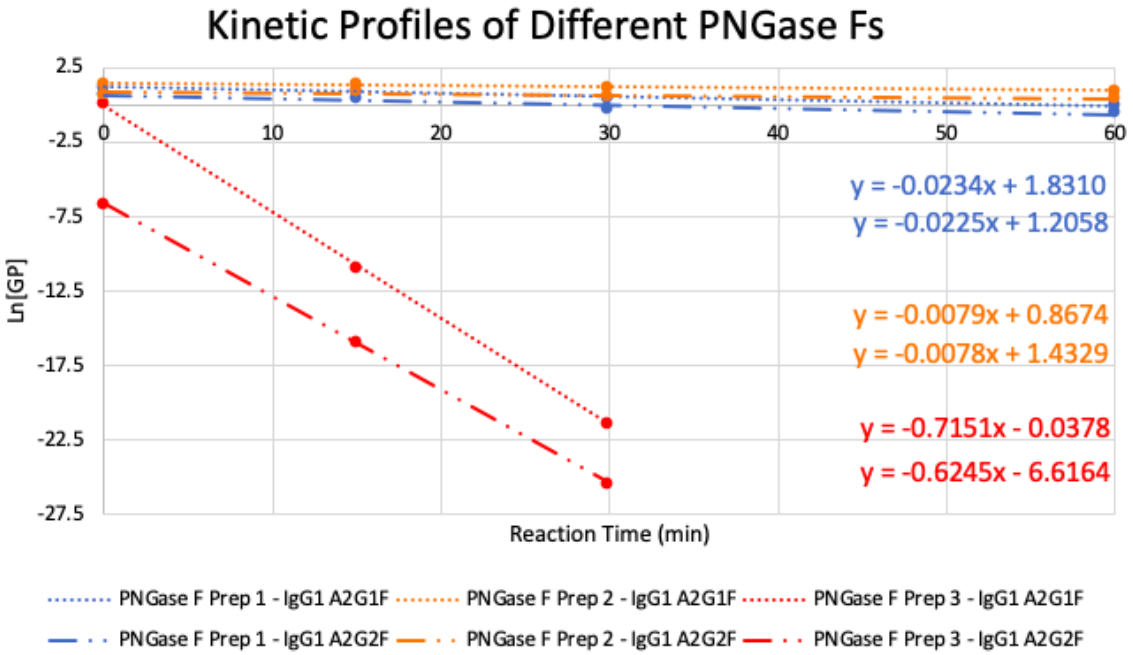

Figure 4. The plot of ln [GP] vs. time for the IgG1 glycopeptide carrying the Fucosylated glycan with 1 galactose (A2G1F) and the IgG1 glycopeptide carrying the Fucosylated glycan with 2 galactoses (A2G2F) deglycosylation for the three PNGase F Preps. This data was obtained following the addition of PNGase F at a concentration of 0.1 U PNGase F/µg IgG. Figure 4 shows the kinetic profile for A2G1F and A2G1F on trypsin digested IgG and PNGase F deglycosylation with PNGase F Prep 1 (in blue), Prep 2 (in orange), and Prep 3 (in red).

Table 1. Average Rate of Deglycosylation for Different PNGase F's Preps Performed on Trypsin Digested IgG Glycopeptides.			
	Rate (k) (Average +/- SD)		
Glycopeptide	PNGase F – Prep 1	PNGase F – Prep 2	PNGase F – Prep 3
IgG1 A2G0N	-	-	0.5250 +/- 0.0550
IgG1 A2G1N	-	-	0.5460 +/- 0.0570
IgG1 A2G2N	-	-	0.6220 +/- 0.0930
IgG1 A2G0F	0.0220 +/- 0.0028	0.0037 +/- 0.0025	0.7820 +/- 0.0250
IgG1 A2G1F	0.0219 +/- 0.0069	0.0030 +/- 0.0014	0.7150 +/- 0.0200
IgG1 A2G2F	0.0202 +/- 0.0064	0.0037 +/- 0.0021	0.6120 +/- 0.0180
IgG1 A2G2F1S1	0.0150 +/- 0.0091	0.0017 +/- 0.0021	0.6050 +/- 0.1920
IgG2/3 A2G2	-	-	-
IgG2/3 A2G0N	0.0253 +/- 0.0021	0.0057 +/- 0.0008	-
IgG2/3 A2G1N	0.0205 +/- 0.0047	0.0031 +/- 0.0019	0.5420 +/- 0.0330
IgG2/3 A2G2N	0.0205 +/- 0.0025	0.0033 +/- 0.0008	0.5590 +/- 0.2860
IgG2/3 A2G0F	0.0051 +/- 0.0015	0.0025 +/- 0.0004	1.0120 +/- 0.3870
IgG2/3 A2G1F	0.0278 +/- 0.0018	0.0056 +/- 0.0024	0.7840 +/- 0.0620
IgG2/3 A2G2F	0.0232 +/- 0.0052	0.0040 +/- 0.0019	0.6540 +/- 0.0830
IgG2/3 A2G2F1S1	-	-	0.3550 +/- 0.2070
IgG4 A2G1	-	-	0.7710 +/- 0.0570
IgG4 A2G2	-	-	-
IgG4 A2G1N	0.0335 +/- 0.0048	0.0024 +/- 0.0016	0.4950 +/- 0.0070
IgG4 A2G0F	0.0205 +/- 0.0058	0.0072 +/- 0.0025	0.4100 +/- 0.0030
IgG4 A2G1F	0.0251 +/- 0.0044	0.0095 +/- 0.0020	0.5620 +/- 0.1370
IgG4 A2G1NF	0.0193 +/- 0.0059	0.0054 +/- 0.0004	0.6040 +/- 0.1120

A dash (-) indicates that the glycopeptide was not observed.

Table 2. Half-life and Time Until Full Deglycosylation on Different PNGase F Deglycosylation Preps						
	Half-life (min)			Time until Full Deglycosylation (min)		
Glycopeptide	Prep 1	Prep 2	Prep 3	Prep 1	Prep 2	Prep 3
IgG1 A2G0	-	-	0.0132	-	-	0.0924
IgG1 A2G1	-	-	0.0127	-	-	0.0888
IgG1 A2G2	-	-	0.0111	-	-	0.0780
IgG1 A2G0N	0.3150	1.8730	0.0089	2.2050	13.1108	0.0620
IgG1 A2G1N	0.3164	2.3100	0.0097	2.2151	16.1700	0.0678
IgG1 A2G2N	0.3431	1.8730	0.0113	2.4015	13.1108	0.0793
IgG1 A2G0F	0.4620	4.0765	0.0115	3.2340	28.5353	0.0802
IgG1 A2G1F	-	-	-	-	-	-
IgG1 A2G2F	0.2739	1.2158	-	1.9174	8.5105	-
IgG1 A2G2F1S1	0.3380	2.2355	0.0128	2.3663	15.6484	0.0895
IgG2/3 A2G2	0.3380	2.1000	0.0124	2.3663	14.7000	0.0868
IgG2/3 A2G0N	1.3588	2.7720	0.0068	9.5118	19.4040	0.0479
IgG2/3 A2G1N	0.2493	1.2375	0.0088	1.7450	8.6625	0.0619
IgG2/3 A2G2N	0.2987	1.7325	0.0106	2.0909	12.1275	0.0742
IgG2/3 A2G0F	-	-	0.0195	-	-	0.1366
IgG2/3 A2G1F	-	-	0.0090	-	-	0.0629
IgG2/3 A2G2F	-	-	-	-	-	-
IgG2/3 A2G2F1S1	0.2069	2.8875	0.0140	1.4481	20.2125	0.0980
IgG4 A2G1	0.3380	0.9625	0.0169	2.3663	6.7375	0.1183
IgG4 A2G2	0.2761	0.7295	0.0123	1.9327	5.1063	0.0863
IgG4 A2G1N	0.3591	1.2833	0.0115	2.5135	8.9833	0.0803
IgG4 A2G0F	-	-	0.0132	-	-	0.0924
IgG4 A2G1F	-	-	0.0127	-	-	0.0888
IgG4 A2G1NF	-	-	0.0111	-	-	0.0780

A dash (-) indicates that the glycopeptide was not observed.

Table 3. Results of Mann-Whitney U Test: Calculating the Significance of Differences in Rates Among Deglycosylation Performed on Tryptic Digested IgGs using Different PNGase F Preps.		
Comparison	**P**	**Result**
k (IgG glycopeptides PNGase F – Prep 1) vs. k (IgG glycopeptides PNGase F – Prep 2)	<0.001	k (IgG glycopeptides PNGase F – Prep 2) < k (IgG glycopeptides PNGase F – Prep 1)
k (IgG glycopeptides PNGase F – Prep 1) vs. k (IgG glycopeptides PNGase F – Prep 3)	<0.001	k (IgG glycopeptides PNGase F – Prep 1) < k (IgG glycopeptides PNGase F – Prep 3)

CHAPTER 7

CONCLUSIONS

Due to their great biological importance, the development of fast and accurate methods to analyze glycoproteins is of the upmost importance. Liquid chromatography paired with mass spectrometry (LC-MS) is a powerful tool for the analysis of glycoproteins, proteins, and glycans. Hydrophilic Interaction Liquid Chromatography (HILIC) is the logical separation method of choice for the analysis of glycopeptides.

The current work presented here utilizes HILIC-LC-MS methods to address various gaps in the field by increasing the depth of information obtained from experiments, including investigating retention behavior, reducing the identification of false positives, and determining kinetics of PNGase F deglycosylation for complete glycan release.

Chapter 3 details the investigation of the HILIC retention behavior of O-mannose glycopeptides. The separation of six O-mannose glycopeptides was observed and the glycopeptides were able to be resolved from each other, and from the native, unmodified peptide. Retention coefficients for O-mannose and extended structures were calculated. The novel separation of GlcNAc linkage isomers in O-mannose glycopeptides was also observed, and the HILIC retention coefficient for both was determined. Retention behavior prediction improves data analysis methods as it allows for quicker data analysis and facilitates the identification of unknowns. The calculation of O-mannose glycan coefficients allows for the prediction of

retention time for any O-mannose glycopeptide consisting of the investigated sugars on any peptide sequence, when combined with previous HILIC peptide retention model.[9]

Chapter 4 highlights that naturally occurring and experimentally induced deamidation of Asn can interfere with the identification of N-linked sites of glycosylation. Thus, shedding light that the current protocol used for glycosylation site mapping can lead to false positives and incorrect assignment of glycosylation sites. To remedy this, the novel HILIC-LC-MS method, n-Asp and i-Asp to reduce false positives (NIFP) was proposed. By this proposed NIFP method, N-linked glycosylation sites can be identified by the presence of an n-Asp residue within the consensus sequence Asn-X-Ser/Thr that also chromatographically shows the presence of one peak, corresponding to Asp. The site is considered to be chemically deamidated if the chromatogram shows the presence of two peaks corresponding to the n-Asp and i-Asp. The intent of this study is to alert investigators in the field to the potential and unexpected errors resulting from this phenomenon and to suggest strategies to overcome this pitfall and prevent the identification of false positives.

Chapter 5 highlights the investigation into solving an age-old question, on whether researchers need to perform a trypsin digest before performing a PNGase F deglycosylation on IgGs. The rate of PNGase F deglycosylation on trypsin digested IgG glycopeptides is 3-4 times faster than on intact IgG, thus the answer to the age-old question is, yes, researchers should perform a trypsin digest before performing a PNGase F deglycosylation on IgGs. The use of a normal amount of PNGase F would digest intact IgG, just at a slower rate. This data suggests that researchers who try to complete a rapid PNGase F glycan release in under 5 minutes may encounter issues with complete deglycosylation. The differences in deglycosylation rate performed on trypsin digested IgGs and intact IgGs suggest that deglycosylation should be

performed on IgGs digested with trypsin to ensure complete deglycosylation in the fastest time to avoid quantitation errors.

Chapter 6 expands on previous research and investigates the kinetics of PNGase F deglycosylation reaction for multiple preps, where three PNGase F enzyme preparations were compared (one amidase and two recombinant versions). The importance of obtaining complete glycan release for accurate quantitation led us to determine if there was a difference in the rate of deglycosylation between the three PNGase F preps. Statistically significant differences in the rate of deglycosylation performed using three different PNGase F enzyme preps on trypsin digested IgGs was determined and the rate of PNGase F deglycosylation with prep 3 deglycosylated IgG tryptic glycopeptides at a rate 34 times faster than prep 1, and PNGase F prep 1 deglycosylated IgG tryptic glycopeptides at a rate 5 times faster than prep 2.

REFERENCES

(1) Reily, C.; Stewart, T. J.; Renfrow, M. B.; Novak, J. Glycosylation in Health and Disease. *Nat Rev Nephrol* **2019**, *15* (6), 346–366. https://doi.org/10.1038/s41581-019-0129-4.

(2) Dwek, M.; Markiv, A. Glycosylation and Disease. In *eLS*; John Wiley & Sons Ltd, Ed.; John Wiley & Sons, Ltd: Chichester, UK, 2018; pp 1–15. https://doi.org/10.1002/9780470015902.a0002151.pub3.

(3) Tian, Y.; Zhang, H. Characterization of Disease-Associated *N* -Linked Glycoproteins. *Proteomics* **2013**, *13* (3–4), 504–511. https://doi.org/10.1002/pmic.201200333.

(4) Vidarsson, G.; Dekkers, G.; Rispens, T. IgG Subclasses and Allotypes: From Structure to Effector Functions. *Front Immunol* **2014**, *5*, 520. https://doi.org/10.3389/fimmu.2014.00520.

(5) Irvine, E. B.; Alter, G. Understanding the Role of Antibody Glycosylation through the Lens of Severe Viral and Bacterial Diseases. *Glycobiology* **2020**, *30* (4), 241–253. https://doi.org/10.1093/glycob/cwaa018.

(6) Arnold, J. N.; Wormald, M. R.; Sim, R. B.; Rudd, P. M.; Dwek, R. A. The Impact of Glycosylation on the Biological Function and Structure of Human Immunoglobulins. *Annu. Rev. Immunol.* **2007**, *25* (1), 21–50. https://doi.org/10.1146/annurev.immunol.25.022106.141702.

(7) Pincetic, A.; Bournazos, S.; DiLillo, D. J.; Maamary, J.; Wang, T. T.; Dahan, R.; Fiebiger, B.-M.; Ravetch, J. V. Type I and Type II Fc Receptors Regulate Innate and Adaptive Immunity. *Nat Immunol* **2014**, *15* (8), 707–716. https://doi.org/10.1038/ni.2939.

(8) Birx, L.; Harvey, A.; Popov, M.; Orlando, R. Reducing Interferences in Glycosylation Site Mapping. *Journal of Biomolecular Techniques* **2022**. https://doi.org/10.7171/3fc1f5fe.7b3a077d.

(9) Badgett, M.; Boyes, B.; Orlando, R. Peptide Retention Prediction Using Hydrophilic Interaction Liquid Chromatography Coupled to Mass Spectrometry. *Journal of Chromatography A* **2018**, *1537*, 58–65.

(10) Ali, I.; Aboul-Enein, H. Y.; Singh, P.; Singh, R.; Sharma, B. Separation of Biological Proteins by Liquid Chromatography. *Saudi Pharm J* **2010**, *18* (2), 59–73. https://doi.org/10.1016/j.jsps.2010.02.001.

(11) Borova, V. L.; Maragou, N. C.; Gago-Ferrero, P.; Pistos, C.; Thomaidis, N. S. Highly Sensitive Determination of 68 Psychoactive Pharmaceuticals, Illicit Drugs, and Related Human Metabolites in Wastewater by Liquid Chromatography–Tandem Mass Spectrometry. *Anal Bioanal Chem* **2014**, *406* (17), 4273–4285. https://doi.org/10.1007/s00216-014-7819-3.

(12) Bagnall, J. P.; Evans, S. E.; Wort, M. T.; Lubben, A. T.; Kasprzyk-Hordern, B. Using Chiral Liquid Chromatography Quadrupole Time-of-Flight Mass Spectrometry for the Analysis of Pharmaceuticals and Illicit Drugs in Surface and Wastewater at the Enantiomeric Level. *Journal of Chromatography A* **2012**, *1249*, 115–129. https://doi.org/10.1016/j.chroma.2012.06.012.

(13) Snyder, L. R. Role of the Solvent in Liquid-Solid Chromatography. Review. *Anal. Chem.* **1974**, *46* (11), 1384–1393. https://doi.org/10.1021/ac60347a052.
(14) Johnson, D.; Boyes, B.; Orlando, R. The Use of Ammonium Formate as a Mobile-Phase Modifier for LC-MS/MS Analysis of Tryptic Digests. *J Biomol Tech* **2013**, *24* (4), 187–197. https://doi.org/10.7171/jbt.13-2404-005.
(15) Rafferty, J. L.; Siepmann, J. I.; Schure, M. R. Mobile Phase Effects in Reversed-Phase Liquid Chromatography: A Comparison of Acetonitrile/Water and Methanol/Water Solvents as Studied by Molecular Simulation. *Journal of Chromatography A* **2011**, *1218* (16), 2203–2213. https://doi.org/10.1016/j.chroma.2011.02.012.
(16) Joseph K. Kirkland; John W. Dolan. *Introduction to Modern Liquid Chromatography*, 3rd ed.; John Wiley & Sons, Ltd, 2010.
(17) Hayes, R.; Ahmed, A.; Edge, T.; Zhang, H. Core–Shell Particles: Preparation, Fundamentals and Applications in High Performance Liquid Chromatography. *Journal of Chromatography A* **2014**, *1357*, 36–52. https://doi.org/10.1016/j.chroma.2014.05.010.
(18) Blue, L. E.; Jorgenson, J. W. 1.1 Mm Superficially Porous Particles for Liquid Chromatography. *Journal of Chromatography A* **2015**, *1380*, 71–80. https://doi.org/10.1016/j.chroma.2014.12.055.
(19) Nawrocki, J. The Silanol Group and Its Role in Liquid Chromatography. *Journal of Chromatography A* **1997**, *779* (1–2), 29–71. https://doi.org/10.1016/S0021-9673(97)00479-2.
(20) Jandera, P. Stationary and Mobile Phases in Hydrophilic Interaction Chromatography: A Review. *Analytica Chimica Acta* **2011**, *692* (1–2), 1–25. https://doi.org/10.1016/j.aca.2011.02.047.
(21) Qiu, H.; Liang, X.; Sun, M.; Jiang, S. Development of Silica-Based Stationary Phases for High-Performance Liquid Chromatography. *Anal Bioanal Chem* **2011**, *399* (10), 3307–3322. https://doi.org/10.1007/s00216-010-4611-x.
(22) Borges, E. M. Silica, Hybrid Silica, Hydride Silica and Non-Silica Stationary Phases for Liquid Chromatography. *Journal of Chromatographic Science* **2015**, *53* (4), 580–597. https://doi.org/10.1093/chromsci/bmu090.
(23) Godinho, J. M.; Naese, J. A.; Toler, A. E.; Boyes, B. E.; Henry, R. A.; DeStefano, J. J.; Grinias, J. P. Importance of Particle Pore Size in Determining Retention and Selectivity in Reversed Phase Liquid Chromatography. *Journal of Chromatography A* **2020**, *1634*, 461678. https://doi.org/10.1016/j.chroma.2020.461678.
(24) JJ Van Deemter; FJ Zuiderwg; A Klinkenberg. Longitudinal Diffusion and Resistance to Mass Transfer as Causes of Non Ideality in Chromatography. *Chem. Eng. Sc.* **1956**, No. 5, 271–289.
(25) Rodrigues, A. E. Permeable Packings and Perfusion Chromatography in Protein Separation. *Journal of Chromatography B: Biomedical Sciences and Applications* **1997**, *699* (1–2), 47–61. https://doi.org/10.1016/S0378-4347(97)00197-7.
(26) Gritti, F.; Guiochon, G. Mass Transfer Kinetics, Band Broadening and Column Efficiency. *Journal of Chromatography A* **2012**, *1221*, 2–40. https://doi.org/10.1016/j.chroma.2011.04.058.
(27) Zou, H.; Zhang, Y.; Hong, M.; Lu, P. Effect of Column Temperature on Retention of Dipeptide Isomers in Reversed-Phase High Performance Liquid Chromatography. *Journal of Liquid Chromatography* **1992**, *15* (13), 2289–2296. https://doi.org/10.1080/10826079208016178.

(28) Edge, T. Turbulent Flow Chromatography in Bioanalysis. In *Handbook of Analytical Separations*; Elsevier, 2003; Vol. 4, pp 91–128. https://doi.org/10.1016/S1567-7192(03)80005-0.
(29) Ettre, L. S. Nomenclature for Chromatography (IUPAC Recommendations 1993). *Pure and Applied Chemistry* **1993**, *65* (4), 819–872. https://doi.org/10.1351/pac199365040819.
(30) Aguilar, M.-I.; Hearn, M. T. W. [1] High-Resolution Reversed-Phase High-Performance Liquid Chromatography of Peptides and Proteins. In *Methods in Enzymology*; Elsevier, 1996; Vol. 270, pp 3–26. https://doi.org/10.1016/S0076-6879(96)70003-4.
(31) Alpert, A. J. Hydrophilic-Interaction Chromatography for the Separation of Peptides, Nucleic Acids and Other Polar Compounds. *Journal of Chromatography A* **1990**, *499*, 177–196. https://doi.org/10.1016/S0021-9673(00)96972-3.
(32) Hemström, P.; Irgum, K. Hydrophilic Interaction Chromatography. *J. Sep. Sci.* **2006**, *29* (12), 1784–1821. https://doi.org/10.1002/jssc.200600199.
(33) Buszewski, B.; Noga, S. Hydrophilic Interaction Liquid Chromatography (HILIC)—a Powerful Separation Technique. *Anal Bioanal Chem* **2012**, *402* (1), 231–247. https://doi.org/10.1007/s00216-011-5308-5.
(34) Cubbon, S.; Bradbury, T.; Wilson, J.; Thomas-Oates, J. Hydrophilic Interaction Chromatography for Mass Spectrometric Metabonomic Studies of Urine. *Anal. Chem.* **2007**, *79* (23), 8911–8918. https://doi.org/10.1021/ac071008v.
(35) Guo, Y.; Gaiki, S. Retention Behavior of Small Polar Compounds on Polar Stationary Phases in Hydrophilic Interaction Chromatography. *Journal of Chromatography A* **2005**, *1074* (1–2), 71–80. https://doi.org/10.1016/j.chroma.2005.03.058.
(36) *High Performance Liquid Chromatography: Fundamental Principles and Practice*, 1st ed.; Lough, W. J., Wainer, I. W., Eds.; Blackie Academic & Professional: London ; New York, 1995.
(37) Scott, R. P. W. *Liquid Chromatography Detectors: Liquid Chromatography Detectors.*; Elsevier Science: Burlington, 2014.
(38) Gevaux, D. Non-Destructive Detection. *Nature Phys* **2014**, *10* (1), 6–6. https://doi.org/10.1038/nphys2867.
(39) Krokhin, O. V.; Ying, S.; Cortens, J. P.; Ghosh, D.; Spicer, V.; Ens, W.; Standing, K. G.; Beavis, R. C.; Wilkins, J. A. Use of Peptide Retention Time Prediction for Protein Identification by Off-Line Reversed-Phase HPLC−MALDI MS/MS. *Anal. Chem.* **2006**, *78* (17), 6265–6269. https://doi.org/10.1021/ac060251b.
(40) Krokhin, O. V.; Ezzati, P.; Spicer, V. Peptide Retention Time Prediction in Hydrophilic Interaction Liquid Chromatography: Data Collection Methods and Features of Additive and Sequence-Specific Models. *Anal. Chem.* **2017**, *89* (10), 5526–5533. https://doi.org/10.1021/acs.analchem.7b00537.
(41) Badgett, M. J.; Mize, E.; Fletcher, T.; Boyes, B.; Orlando, R. Predicting the HILIC Retention Behavior of the N-Linked Glycopeptides Produced by Trypsin Digestion of Immunoglobulin Gs (IgGs). *J Biomol Tech* **2018**, *29* (4), 98–104. https://doi.org/10.7171/jbt.18-2904-002.
(42) Badgett, M. J.; Boyes, B.; Orlando, R. The Separation and Quantitation of Peptides with and without Oxidation of Methionine and Deamidation of Asparagine Using Hydrophilic Interaction Liquid Chromatography with Mass Spectrometry (HILIC-MS). *J. Am. Soc. Mass Spectrom.* **2017**, *28* (5), 818–826. https://doi.org/10.1007/s13361-016-1565-z.

(43) Krokhin, O. V.; Spicer, V. Peptide Retention Standards and Hydrophobicity Indexes in Reversed-Phase High-Performance Liquid Chromatography of Peptides. *Anal. Chem.* **2009**, *81* (22), 9522–9530. https://doi.org/10.1021/ac9016693.
(44) Han, X.; Aslanian, A.; Yates, J. R. Mass Spectrometry for Proteomics. *Curr Opin Chem Biol* **2008**, *12* (5), 483–490. https://doi.org/10.1016/j.cbpa.2008.07.024.
(45) Ho, C. S.; Lam, C. W. K.; Chan, M. H. M.; Cheung, R. C. K.; Law, L. K.; Lit, L. C. W.; Ng, K. F.; Suen, M. W. M.; Tai, H. L. Electrospray Ionisation Mass Spectrometry: Principles and Clinical Applications. *Clin Biochem Rev* **2003**, *24* (1), 3–12.
(46) Chowdhury, S. K.; Katta, V.; Chait, B. T. Electrospray Ionization Mass Spectrometric Peptide Mapping: A Rapid, Sensitive Technique for Protein Structure Analysis. *Biochemical and Biophysical Research Communications* **1990**, *167* (2), 686–692. https://doi.org/10.1016/0006-291X(90)92080-J.
(47) Fenn, J. B.; Mann, M.; Meng, C. K.; Wong, S. F.; Whitehouse, C. M. Electrospray Ionization for Mass Spectrometry of Large Biomolecules. *Science* **1989**, *246* (4926), 64–71. https://doi.org/10.1126/science.2675315.
(48) Singhal, N.; Kumar, M.; Kanaujia, P. K.; Virdi, J. S. MALDI-TOF Mass Spectrometry: An Emerging Technology for Microbial Identification and Diagnosis. *Front. Microbiol.* **2015**, *6*. https://doi.org/10.3389/fmicb.2015.00791.
(49) Leopold, J.; Popkova, Y.; Engel, K.; Schiller, J. Recent Developments of Useful MALDI Matrices for the Mass Spectrometric Characterization of Lipids. *Biomolecules* **2018**, *8* (4), 173. https://doi.org/10.3390/biom8040173.
(50) Villas-Bôas, S. G.; Mas, S.; Åkesson, M.; Smedsgaard, J.; Nielsen, J. Mass Spectrometry in Metabolome Analysis. *Mass Spectrom. Rev.* **2005**, *24* (5), 613–646. https://doi.org/10.1002/mas.20032.
(51) Hoffmann, E. de; Stroobant, V. *Mass Spectrometry: Principles and Applications*, 2nd ed.; Wiley: Chichester ; New York, 2001.
(52) Paul, W. Electromagnetic Traps for Charged and Neutral Particles. *Rev. Mod. Phys.* **1990**, *62* (3), 531–540. https://doi.org/10.1103/RevModPhys.62.531.
(53) Yates, J. R.; Cociorva, D.; Liao, L.; Zabrouskov, V. Performance of a Linear Ion Trap-Orbitrap Hybrid for Peptide Analysis. *Anal. Chem.* **2006**, *78* (2), 493–500. https://doi.org/10.1021/ac0514624.
(54) Cavaliere, C.; Antonelli, M.; Capriotti, A. L.; La Barbera, G.; Montone, C. M.; Piovesana, S.; Laganà, A. A Triple Quadrupole and a Hybrid Quadrupole Orbitrap Mass Spectrometer in Comparison for Polyphenol Quantitation. *J. Agric. Food Chem.* **2019**, *67* (17), 4885–4896. https://doi.org/10.1021/acs.jafc.8b07163.
(55) Hocart, C. H. Mass Spectrometry: An Essential Tool for Trace Identification and Quantification. In *Comprehensive Natural Products II*; Elsevier, 2010; pp 327–388. https://doi.org/10.1016/B978-008045382-8.00187-8.
(56) Douglas, D. J.; Frank, A. J.; Mao, D. Linear Ion Traps in Mass Spectrometry. *Mass Spectrom. Rev.* **2005**, *24* (1), 1–29. https://doi.org/10.1002/mas.20004.
(57) B. A. Mamyrin; V. I. Karataev; D. V. Shmikk; V. A. Zagulin. The Mass-Reflectron, a New Nonmagnetic Time-of-Flight Mass Spectrometer with High Resolution. *Zh. Eksp. Teor. Fiz.* **1972**, No. 64, 82–89.
(58) Boesl, U. Time-of-Flight Mass Spectrometry: Introduction to the Basics: TIME-OF-FLIGHT MASS SPECTROMETRY. *Mass Spec Rev* **2017**, *36* (1), 86–109. https://doi.org/10.1002/mas.21520.

(59) Grix, R.; Kutscher, R.; Li, G.; Grüner, U.; Wollnik, H.; Matsuda, H. A Time-of-Flight Mass Analyzer with High Resolving Power. *Rapid Commun. Mass Spectrom.* **1988**, *2* (5), 83–85. https://doi.org/10.1002/rcm.1290020503.
(60) Shukla, A. K.; Futrell, J. H. Tandem Mass Spectrometry: Dissociation of Ions by Collisional Activation. *J. Mass Spectrom.* **2000**, *35* (9), 1069–1090. https://doi.org/10.1002/1096-9888(200009)35:9<1069::AID-JMS54>3.0.CO;2-C.
(61) Juang, Y.-M.; She, T.-F.; Chen, H.-Y.; Lai, C.-C. Comparison of CID versus ETD-Based MS/MS Fragmentation for the Analysis of Doubly Derivatized Steroids: CID versus ETD for Steroids. *J. Mass Spectrom.* **2013**, *48* (12), 1349–1356. https://doi.org/10.1002/jms.3300.
(62) Frenich, A. G.; Plaza-Bolaños, P.; Vidal, J. L. M. Comparison of Tandem-in-Space and Tandem-in-Time Mass Spectrometry in Gas Chromatography Determination of Pesticides: Application to Simple and Complex Food Samples. *Journal of Chromatography A* **2008**, *1203* (2), 229–238. https://doi.org/10.1016/j.chroma.2008.07.041.
(63) Johnson, J. V.; Yost, R. A.; Kelley, P. E.; Bradford, D. C. Tandem-in-Space and Tandem-in-Time Mass Spectrometry: Triple Quadrupoles and Quadrupole Ion Traps. *Anal. Chem.* **1990**, *62* (20), 2162–2172. https://doi.org/10.1021/ac00219a003.
(64) Dass, C. *Fundamentals of Contemporary Mass Spectrometry*; Wiley-Interscience: Hoboken, N.J., 2007.
(65) Yost, R. A.; Enke, C. G. Selected Ion Fragmentation with a Tandem Quadrupole Mass Spectrometer. *J. Am. Chem. Soc.* **1978**, *100* (7), 2274–2275. https://doi.org/10.1021/ja00475a072.
(66) Chernushevich, I. V.; Loboda, A. V.; Thomson, B. A. An Introduction to Quadrupole-Time-of-Flight Mass Spectrometry. *J. Mass Spectrom.* **2001**, *36* (8), 849–865. https://doi.org/10.1002/jms.207.
(67) Tao, S.; Chan, H.; van der Graaf, H. Secondary Electron Emission Materials for Transmission Dynodes in Novel Photomultipliers: A Review. *Materials* **2016**, *9* (12), 1017. https://doi.org/10.3390/ma9121017.
(68) Burroughs, E. G. Collection Efficiency of Continuous Dynode Electron Multiple Arrays. *Review of Scientific Instruments* **1969**, *40* (1), 35–37. https://doi.org/10.1063/1.1683743.
(69) Ladislas Wiza, J. Microchannel Plate Detectors. *Nuclear Instruments and Methods* **1979**, *162* (1–3), 587–601. https://doi.org/10.1016/0029-554X(79)90734-1.
(70) Ireland, T. R. Ion Microscopes and Microprobes. In *Treatise on Geochemistry*; Elsevier, 2014; pp 385–409. https://doi.org/10.1016/B978-0-08-095975-7.01430-3.
(71) Ramazi, S.; Zahiri, J. Post-Translational Modifications in Proteins: Resources, Tools and Prediction Methods. *Database* **2021**, *2021*, baab012. https://doi.org/10.1093/database/baab012.
(72) An, H. J.; Froehlich, J. W.; Lebrilla, C. B. Determination of Glycosylation Sites and Site-Specific Heterogeneity in Glycoproteins. *Current Opinion in Chemical Biology* **2009**, *13* (4), 421–426. https://doi.org/10.1016/j.cbpa.2009.07.022.
(73) Apweiler, R. On the Frequency of Protein Glycosylation, as Deduced from Analysis of the SWISS-PROT Database. *Biochimica et Biophysica Acta (BBA) - General Subjects* **1999**, *1473* (1), 4–8. https://doi.org/10.1016/S0304-4165(99)00165-8.
(74) *Essentials of Glycobiology*, 2nd ed.; Varki, A., Ed.; Cold Spring Harbor Laboratory Press: Cold Spring Harbor, N.Y, 2009.

(75) Stanley, T.; Taniguchi, N. N-Glycans [Chapter 9]. In *Essentials of Glycobiology*; Cold Spring Harbor Laboratory: Cold Spring Harbor (NY), 2017.
(76) Hang, H. C.; Bertozzi, C. R. The Chemistry and Biology of Mucin-Type O-Linked Glycosylation. *Bioorganic & Medicinal Chemistry* **2005**, *13* (17), 5021–5034. https://doi.org/10.1016/j.bmc.2005.04.085.
(77) Ma, J.; Hart, G. W. Protein *O* -GlcNAcylation in Diabetes and Diabetic Complications. *Expert Review of Proteomics* **2013**, *10* (4), 365–380. https://doi.org/10.1586/14789450.2013.820536.
(78) Wells, L. The O-Mannosylation Pathway: Glycosyltransferases and Proteins Implicated in Congenital Muscular Dystrophy. *Journal of Biological Chemistry* **2013**, *288* (10), 6930–6935. https://doi.org/10.1074/jbc.R112.438978.
(79) Stanley, P.; Guidos, C. J. Regulation of Notch Signaling during T- and B-Cell Development by *O* -Fucose Glycans. *Immunological Reviews* **2009**, *230* (1), 201–215. https://doi.org/10.1111/j.1600-065X.2009.00791.x.
(80) Kiyoshi, M.; Tsumoto, K.; Ishii-Watabe, A.; Caaveiro, J. M. M. Glycosylation of IgG-Fc: A Molecular Perspective. *International Immunology* **2017**, *29* (7), 311–317. https://doi.org/10.1093/intimm/dxx038.
(81) Gudelj, I.; Lauc, G.; Pezer, M. Immunoglobulin G Glycosylation in Aging and Diseases. *Cellular Immunology* **2018**, *333*, 65–79. https://doi.org/10.1016/j.cellimm.2018.07.009.
(82) Raju, T. S. Terminal Sugars of Fc Glycans Influence Antibody Effector Functions of IgGs. *Current Opinion in Immunology* **2008**, *20* (4), 471–478. https://doi.org/10.1016/j.coi.2008.06.007.
(83) Yehuda, S.; Padler-Karavani, V. Glycosylated Biotherapeutics: Immunological Effects of N-Glycolylneuraminic Acid. *Front. Immunol.* **2020**, *11*, 21. https://doi.org/10.3389/fimmu.2020.00021.
(84) Kim, J. Y.; Kim, Y.-G.; Lee, G. M. CHO Cells in Biotechnology for Production of Recombinant Proteins: Current State and Further Potential. *Appl Microbiol Biotechnol* **2012**, *93* (3), 917–930. https://doi.org/10.1007/s00253-011-3758-5.
(85) Ghaderi, D.; Zhang, M.; Hurtado-Ziola, N.; Varki, A. Production Platforms for Biotherapeutic Glycoproteins. Occurrence, Impact, and Challenges of Non-Human Sialylation. *Biotechnology and Genetic Engineering Reviews* **2012**, *28* (1), 147–176. https://doi.org/10.5661/bger-28-147.
(86) Ghaderi, D.; Taylor, R. E.; Padler-Karavani, V.; Diaz, S.; Varki, A. Implications of the Presence of N-Glycolylneuraminic Acid in Recombinant Therapeutic Glycoproteins. *Nat Biotechnol* **2010**, *28* (8), 863–867. https://doi.org/10.1038/nbt.1651.
(87) Altman, M. O.; Gagneux, P. Absence of Neu5Gc and Presence of Anti-Neu5Gc Antibodies in Humans—An Evolutionary Perspective. *Front. Immunol.* **2019**, *10*, 789. https://doi.org/10.3389/fimmu.2019.00789.
(88) Hilger, C.; Fischer, J.; Wölbing, F.; Biedermann, T. Role and Mechanism of Galactose-Alpha-1,3-Galactose in the Elicitation of Delayed Anaphylactic Reactions to Red Meat. *Curr Allergy Asthma Rep* **2019**, *19* (1), 3. https://doi.org/10.1007/s11882-019-0835-9.
(89) Ayoub, D.; Jabs, W.; Resemann, A.; Evers, W.; Evans, C.; Main, L.; Baessmann, C.; Wagner-Rousset, E.; Suckau, D.; Beck, A. Correct Primary Structure Assessment and Extensive Glyco-Profiling of Cetuximab by a Combination of Intact, Middle-up, Middle-down and Bottom-up ESI and MALDI Mass Spectrometry Techniques. *mAbs* **2013**, *5* (5), 699–710. https://doi.org/10.4161/mabs.25423.

(90) Platts-Mills, T. A. E.; Commins, S. P.; Biedermann, T.; van Hage, M.; Levin, M.; Beck, L. A.; Diuk-Wasser, M.; Jappe, U.; Apostolovic, D.; Minnicozzi, M.; Plaut, M.; Wilson, J. M. On the Cause and Consequences of IgE to Galactose-α-1,3-Galactose: A Report from the National Institute of Allergy and Infectious Diseases Workshop on Understanding IgE-Mediated Mammalian Meat Allergy. *Journal of Allergy and Clinical Immunology* **2020**, *145* (4), 1061–1071. https://doi.org/10.1016/j.jaci.2020.01.047.

(91) Moradian, A.; Kalli, A.; Sweredoski, M. J.; Hess, S. The Top-down, Middle-down, and Bottom-up Mass Spectrometry Approaches for Characterization of Histone Variants and Their Post-Translational Modifications. *Proteomics* **2014**, *14* (4–5), 489–497. https://doi.org/10.1002/pmic.201300256.

(92) Shajahan, A.; Heiss, C.; Ishihara, M.; Azadi, P. Glycomic and Glycoproteomic Analysis of Glycoproteins—a Tutorial. *Anal Bioanal Chem* **2017**, *409* (19), 4483–4505. https://doi.org/10.1007/s00216-017-0406-7.

(93) Imre, T.; Schlosser, G.; Pocsfalvi, G.; Siciliano, R.; Molnár-Szöllősi, É.; Kremmer, T.; Malorni, A.; Vékey, K. Glycosylation Site Analysis of Human Alpha-1-Acid Glycoprotein (AGP) by Capillary Liquid Chromatography—Electrospray Mass Spectrometry. *J. Mass Spectrom.* **2005**, *40* (11), 1472–1483. https://doi.org/10.1002/jms.938.

(94) Hale, J. E.; Butler, J. P.; Gelfanova, V.; You, J.-S.; Knierman, M. D. A Simplified Procedure for the Reduction and Alkylation of Cysteine Residues in Proteins Prior to Proteolytic Digestion and Mass Spectral Analysis. *Analytical Biochemistry* **2004**, *333* (1), 174–181. https://doi.org/10.1016/j.ab.2004.04.013.

(95) Chen, R.; Jiang, X.; Sun, D.; Han, G.; Wang, F.; Ye, M.; Wang, L.; Zou, H. Glycoproteomics Analysis of Human Liver Tissue by Combination of Multiple Enzyme Digestion and Hydrazide Chemistry. *J. Proteome Res.* **2009**, *8* (2), 651–661. https://doi.org/10.1021/pr8008012.

(96) Tsiatsiani, L.; Heck, A. J. R. Proteomics beyond Trypsin. *FEBS J* **2015**, *282* (14), 2612–2626. https://doi.org/10.1111/febs.13287.

(97) Huddleston, M. J.; Bean, M. F.; Carr, S. A. Collisional Fragmentation of Glycopeptides by Electrospray Ionization LC/MS and LC/MS/MS: Methods for Selective Detection of Glycopeptides in Protein Digests. *Anal. Chem.* **1993**, *65* (7), 877–884. https://doi.org/10.1021/ac00055a009.

(98) Conboy, J. J.; Henion, J. D. The Determination of Glycopeptides by Liquid Chromatography/Mass Spectrometry with Collision-Induced Dissociation. *J. Am. Soc. Mass Spectrom.* **1992**, *3* (8), 804–814. https://doi.org/10.1016/1044-0305(92)80003-4.

(99) Domon, B.; Costello, C. E. A Systematic Nomenclature for Carbohydrate Fragmentations in FAB-MS/MS Spectra of Glycoconjugates. *Glycoconjugate J* **1988**, *5* (4), 397–409. https://doi.org/10.1007/BF01049915.

(100) Leymarie, N.; Zaia, J. Effective Use of Mass Spectrometry for Glycan and Glycopeptide Structural Analysis. *Anal. Chem.* **2012**, *84* (7), 3040–3048. https://doi.org/10.1021/ac3000573.

(101) Veillon, L.; Huang, Y.; Peng, W.; Dong, X.; Cho, B. G.; Mechref, Y. Characterization of Isomeric Glycan Structures by LC-MS/MS: Liquid Phase Separations. *ELECTROPHORESIS* **2017**, *38* (17), 2100–2114. https://doi.org/10.1002/elps.201700042.

(102) Sheikh, M. O.; Halmo, S. M.; Wells, L. Recent Advancements in Understanding Mammalian O-Mannosylation. *Glycobiology* **2017**, *27* (9), 806–819. https://doi.org/10.1093/glycob/cwx062.
(103) Praissman, J. L.; Willer, T.; Sheikh, M. O.; Toi, A.; Chitayat, D.; Lin, Y.-Y.; Lee, H.; Stalnaker, S. H.; Wang, S.; Prabhakar, P. K.; Nelson, S. F.; Stemple, D. L.; Moore, S. A.; Moremen, K. W.; Campbell, K. P.; Wells, L. The Functional O-Mannose Glycan on α-Dystroglycan Contains a Phospho-Ribitol Primed for Matriglycan Addition. *eLife* **2016**, *5*, e14473. https://doi.org/10.7554/eLife.14473.
(104) Neubert, P.; Halim, A.; Zauser, M.; Essig, A.; Joshi, H. J.; Zatorska, E.; Larsen, I. S. B.; Loibl, M.; Castells-Ballester, J.; Aebi, M.; Clausen, H.; Strahl, S. Mapping the O-Mannose Glycoproteome in Saccharomyces Cerevisiae. *Molecular & Cellular Proteomics* **2016**, *15* (4), 1323–1337. https://doi.org/10.1074/mcp.M115.057505.
(105) Praissman, J. L.; Wells, L. Mammalian O-Mannosylation Pathway: Glycan Structures, Enzymes, and Protein Substrates. *Biochemistry* **2014**, *53* (19), 3066–3078. https://doi.org/10.1021/bi500153y.
(106) Mariño, K.; Bones, J.; Kattla, J. J.; Rudd, P. M. A Systematic Approach to Protein Glycosylation Analysis: A Path through the Maze. *Nat Chem Biol* **2010**, *6* (10), 713–723. https://doi.org/10.1038/nchembio.437.
(107) Huang, Y.; Nie, Y.; Boyes, B.; Orlando, R. Resolving Isomeric Glycopeptide Glycoforms with Hydrophilic Interaction Chromatography (HILIC). *J Biomol Tech* **2016**, *27* (3), 98–104. https://doi.org/10.7171/jbt.16-2703-003.
(108) Badgett, M. J.; Boyes, B.; Orlando, R. Predicting the Retention Behavior of Specific O-Linked Glycopeptides. *J Biomol Tech* **2017**, *28* (3), 122–126. https://doi.org/10.7171/jbt.17-2803-003.
(109) Halmo, S. M.; Singh, D.; Patel, S.; Wang, S.; Edlin, M.; Boons, G.-J.; Moremen, K. W.; Live, D.; Wells, L. Protein O-Linked Mannose β-1,4-N-Acetylglucosaminyl-Transferase 2 (POMGNT2) Is a Gatekeeper Enzyme for Functional Glycosylation of α-Dystroglycan. *Journal of Biological Chemistry* **2017**, *292* (6), 2101–2109. https://doi.org/10.1074/jbc.M116.764712.
(110) MacLean, B.; Tomazela, D. Skyline: An Open Source Document Editor for Creating and Analyzing Targeted Proteomics Experiments. *Bioinformatics* **2010**, *26* (7), 966–968.
(111) Brockhausen, I. *Glycobiology Protocols*; Methods in molecular biology; Humana press: Totowa (N.J.), 2006.
(112) Kozlik, P.; Goldman, R.; Sanda, M. Hydrophilic Interaction Liquid Chromatography in the Separation of Glycopeptides and Their Isomers. *Anal Bioanal Chem* **2018**, *410* (20), 5001–5008. https://doi.org/10.1007/s00216-018-1150-3.
(113) Neidleman, S. L.; Laskin, A. I. *Advances in Applied Microbiology. Volume 44 Volume 44*; Academic Press: New York, 1997.
(114) Badgett, M.; Boyes, B.; Orlando, R. Peptide Retention Prediction Using Hydrophilic Interaction Liquid Chromatography Coupled to Mass Spectrometry. *Journal of Chromatography A* **2018**, *1537*, 58–65.
(115) Nakagawa, H.; Hato, M. Detection of Altered N-Glycans Profiles in Whole Serum from Rheumatoid Arthritis Patients. *Journal of Chromatography B* **2007**, *853* (1–2), 133–137.
(116) Bermingham, M.; Colombo, M. N-Glycan Profile and Kidney Disease in Type 1 Diabetes. *Diabetes Care* **2018**, *41* (1), 79–87.

(117) Trbojevic Akmacic, I.; Ventham, N. Inflammatory Bowel Disease Associates with Proinflammatory Potential of the Immunoglobulin G Glycome. *Inflammatory Bowel Diesease* **2015**, *21* (6), 1237–1247.
(118) Kodar, K.; Stadlmann, J.; Klaamas, K. Immunoglobulin G Fc N-Glycan Profiling in Patients with Gastric Cancer by LC-ESI-MS:Relation to Tumor Progression and Survival. *Glycoconjugate Journal* **2012**, *29* (1), 57–66.
(119) Chen, G.; Wang, Y.; Qin, X. Change in IgG1 Fc N-Linked Glycosylation in Human Lung Cancer: Age- and Sex-Related Diagnostic Potential. *Electrophoresis* **2013**, *34* (16), 2407–2416.
(120) Ren, D.; Pipes, G.; Liu, D. An Improved Trypsin Digestion Method Minimizes Digestion-Induced Modfication on Proteins. *Analytical Biochemistry* **2009**, *392*, 12–21.
(121) Geiger, T.; Clarke, S. Deamidation, Isomerization, and Racemization at Asparaginyl and Aspartyl Residues in Peptides. Succinimide-Linked Reactions That Contribute to Protein Degradation. *J. Biol. Chem.* **1987**, *262*, 785–794.
(122) Roher, A.; Lowenson, J.; Clarke, S. Structural Alterations in the Peptide Backbone of Beta-Amyloid Core Protein May Account for Its Deposition and Stability in Alzheimer's Disease. *J. Biol. Chem.* **1993**, *268*, 3072–3083.
(123) Takata, T.; Oxford, J.; Demeler, B. Deamidation Destabilizes and Triggers Aggregation of a Lens Protein, BetaA3-Crystallin. *Protein Sci.* **2008**, *17*, 1565–1575.
(124) Wilmarth, P.; Tanner, S.; Dasari, S. Age-Related Changes in Human Crystallins Determined from Comparative Analysis of Post-Translational Modifications in Young and Aged Lens: Does Deamidation Contribute to Crystallin Insolubility? *J. Proteome Res.* **2006**, *5*, 2554–2566.
(125) Robinson, N. E.; Robinson, A. B. Amide Molecular Clocks in Drosophilia Proteins: Potential Regulators of Aging and Other Processes. *Mech. Ageing Dev.* **2004**, *125*, 259–267.
(126) Robinson, N. E.; Robinson, A. B. Molecular Clocks. *Proc. Natl. Acad. Sci.* **2001**, *98*, 944–949.
(127) Bischoff, R.; Kolbe, H. V. J. Deamidation of Asparagine and Glutamine Residues in Proteins and Peptides: Structural Determinants and Analytical Methodology. *Journal of Chromatography B: Biomedical Sciences and Applications* **1994**, *662* (2), 261–278. https://doi.org/10.1016/0378-4347(94)00203-7.
(128) Catak, S.; Monard, G.; Aviyente, V.; Ruiz-López, M. F. Deamidation of Asparagine Residues: Direct Hydrolysis versus Succinimide-Mediated Deamidation Mechanisms. *J. Phys. Chem. A* **2009**, *113* (6), 1111–1120. https://doi.org/10.1021/jp808597v.
(129) Tyler-Cross, R.; Schirch, V. Effects of Amino Acid Sequence, Buffers, and Ionic Strength on the Rate and Mechanism of Deamidation of Asparagine Resides in Small Peptides. *J. Biol. Chem.* **1991**, *266* (33), 22549–22556.
(130) Robinson, N. E.; Robinson, A. B. Prediction of Protein Deamidation Rates from Primary and Three-Dimensional Structure. *Proceedings of the National Academy of Sciences* **2001**, *98* (8), 4367–4372. https://doi.org/10.1073/pnas.071066498.
(131) Robinson, N. E. Protein Deamidation. *Proceedings of the National Academy of Sciences* **2002**, *99* (8), 5283–5288. https://doi.org/10.1073/pnas.082102799.
(132) Sydow, J. F.; Lipsmeier, F.; Larraillet, V.; Hilger, M.; Mautz, B.; Mølhøj, M.; Kuentzer, J.; Klostermann, S.; Schoch, J.; Voelger, H. R.; Regula, J. T.; Cramer, P.; Papadimitriou, A.; Kettenberger, H. Structure-Based Prediction of Asparagine and Aspartate

Degradation Sites in Antibody Variable Regions. *PLoS ONE* **2014**, *9* (6), e100736. https://doi.org/10.1371/journal.pone.0100736.
(133) Wright, H. Nonenzymatic Deamidation of Asparaginyl and Glutaminyl Residues in Proteins. *Crit. Reb. Biochem. Mol. Biol.* **1991**, *26* (1), 1–52.
(134) Tarentino, A.; Gomez, C.; Plummer, T. Deglycosylation of Asparagine-Linked Glycans by Peptide:N-Glycosidase. *Biochemistry* **1985**, *24* (17), 4665–4671.
(135) Hirani, S.; Bernasconi, R.; Rasmussen, J. R. Use of N-Glycanase to Release Asparagine-Linked Oligosaccharides for Structural Analysis. *Analytical Biochemistry* **1987**, *162* (2), 485–492.
(136) *UniProtKB - P01857 (IGHG1_HUMAN)*. https://www.uniprot.org/uniprot/P01857.
(137) Tarentino, A. L.; Quinones, G.; Trumble, A.; Changchien, L. M.; Duceman, B.; Maley, F.; Plummer, T. H. Molecular Cloning and Amino Acid Sequence of Peptide-N4-(N-Acetyl-Beta-D-Glucosaminyl)Asparagine Amidase from Flavobacterium Meningosepticum. *J Biol Chem* **1990**, *265* (12), 6961–6966.
(138) Tarentino, A. L.; Trimble, R. B.; Plummer, T. H. Chapter 5 Enzymatic Approaches for Studying the Structure, Synthesis, and Processing of Glycoproteins. In *Methods in Cell Biology*; Elsevier, 1989; Vol. 32, pp 111–139. https://doi.org/10.1016/S0091-679X(08)61169-3.
(139) Sun, G.; Yu, X.; Bao, C.; Wang, L.; Li, M.; Gan, J.; Qu, D.; Ma, J.; Chen, L. Identification and Characterization of a Novel Prokaryotic Peptide. *Journal of Biological Chemistry* **2015**, *290* (12), 7452–7462. https://doi.org/10.1074/jbc.M114.605493.
(140) An, H. J.; Froehlich, J. W.; Lebrilla, C. B. Determination of Glycosylation Sites and Site-Specific Heterogeneity in Glycoproteins. *Current Opinion in Chemical Biology* **2009**, *13* (4), 421–426. https://doi.org/10.1016/j.cbpa.2009.07.022.
(141) Nishiyama, T.; Kimura, N.; Jitsuhara, Y.; Uchida, M.; Ochi, F.; Yamaguchi, H. N-Glycans Protect Proteins from Protease Digestion through Their Binding Affinities for Aromatic Amino Acid Residues. *J Biochem* **2000**, *127* (3), 427–433. https://doi.org/10.1093/oxfordjournals.jbchem.a022624.
(142) Petrucci, R. H. *General Chemistry: Principles and Modern Applications*, 9th ed.; Pearson/Prentice Hall: Upper Saddle River, N.J, 2007.
(143) Conover, W. J. *Practical Nonparametric Statistics*, 3rd ed.; Wiley series in probability and statistics. Applied probability and statistics section; Wiley: New York, 1999.
(144) Rebecca Duke; Christopher Taron. N-Glycan Composition Profiling for Quality Testing of Biotherapeutics. *Biopharm International* **2015**, *28*.
(145) Zhou, H.; Briscoe, A. C.; Froehlich, J. W.; Lee, R. S. PNGase F Catalyzes De-N-Glycosylation in a Domestic Microwave. *Analytical Biochemistry* **2012**, *427* (1), 33–35. https://doi.org/10.1016/j.ab.2012.04.011.
(146) Krenkova, J.; Szekrenyes, A.; Keresztessy, Z.; Foret, F.; Guttman, A. Oriented Immobilization of Peptide-N-Glycosidase F on a Monolithic Support for Glycosylation Analysis. *Journal of Chromatography A* **2013**, *1322*, 54–61. https://doi.org/10.1016/j.chroma.2013.10.087.
(147) Huang, Y.; Orlando, R. Kinetics of N-Glycan Release from Human Immunoglobulin G (IgG) by PNGase F: All Glycans Are Not Created Equal. *J Biomol Tech* **2017**, *28* (4), 150–157. https://doi.org/10.7171/jbt.17-2804-002.